

# An adaptive high-dimensional stochastic model representation technique for the solution of stochastic partial differential equations

Xiang Ma, Nicholas Zabaras \*

Materials Process Design and Control Laboratory, Sibley School of Mechanical and Aerospace Engineering, 101 Frank H.T. Rhodes Hall, Cornell University, Ithaca, NY 14853-3801, USA

## ARTICLE INFO

### Article history:

Received 9 July 2009

Received in revised form 20 January 2010

Accepted 25 January 2010

Available online 1 February 2010

### Keywords:

Stochastic partial differential equations

High-dimensional model representation

Stochastic collocation method

Sparse grids

Random heterogeneous media

## ABSTRACT

A computational methodology is developed to address the solution of high-dimensional stochastic problems. It utilizes high-dimensional model representation (HDMR) technique in the stochastic space to represent the model output as a finite hierarchical correlated function expansion in terms of the stochastic inputs starting from lower-order to higher-order component functions. HDMR is efficient at capturing the high-dimensional input–output relationship such that the behavior for many physical systems can be modeled to good accuracy only by the first few lower-order terms. An adaptive version of HDMR is also developed to automatically detect the important dimensions and construct higher-order terms using only the important dimensions. The newly developed adaptive sparse grid collocation (ASGC) method is incorporated into HDMR to solve the resulting sub-problems. By integrating HDMR and ASGC, it is computationally possible to construct a low-dimensional stochastic reduced-order model of the high-dimensional stochastic problem and easily perform various statistic analysis on the output. Several numerical examples involving elementary mathematical functions and fluid mechanics problems are considered to illustrate the proposed method. The cases examined show that the method provides accurate results for stochastic dimensionality as high as 500 even with large-input variability. The efficiency of the proposed method is examined by comparing with Monte Carlo (MC) simulation.

© 2010 Elsevier Inc. All rights reserved.

## 1. Introduction

Over the past few decades there has been considerable interest among the scientific community in studying physical processes with stochastic inputs. These stochastic input conditions arise from uncertainties in boundary and initial conditions as well as from inherent random material heterogeneities. Material heterogeneities are usually difficult to quantify since it is physically impossible to know the exact property at every point in the domain. In most cases, only a few statistical descriptors of the property variation or the property variation in small test regions can be experimentally determined. This limited information necessitates viewing the property variation as a random field that satisfies certain statistical properties/correlations. Several techniques, such as Karhunen–Loève (K-L) expansion [1] and model reduction methods [2,3] have been proposed to generate these stochastic input models. This naturally results in describing the physical phenomena using stochastic partial differential equations (SPDEs).

\* Corresponding author. Fax: +1 607 255 1222.

E-mail address: [zabaras@cornell.edu](mailto:zabaras@cornell.edu) (N. Zabaras).

URL: <http://mpdc.mae.cornell.edu/> (N. Zabaras).

In the past decade, there has been tremendous progress in posing and solving SPDEs with the methods used usually classified into three major groups. The first group refers to sampling methods. The most traditional one is the Monte Carlo (MC) method. Its convergence rate does not depend on the number of independent input random variables. Furthermore, MC methods are very easy to implement given a working deterministic code. However, the number of realizations required to acquire good statistics is usually quite large. The second group of methods consists of moment/perturbation methods, e.g. KL-based moment-equation approach [4–6]. These methods can deal with large number of inputs. However, they are limited to small fluctuations and do not provide high-order statistics of the solution. Significant emphasis is given recently on the non-perturbative methods. The first approach in this group for quantifying uncertainty is the spectral stochastic finite element method (SSFEM) [1] based on generalized polynomial chaos expansions (gPC) [7]. In this method, we project the dependent variables of the model onto a stochastic space spanned by a set of complete orthogonal polynomials and then a Galerkin projection scheme is used to transform the original stochastic problem into a system of coupled deterministic equations which can be solved by the finite element method. The gPC was successfully applied to model uncertainty propagation in random heterogeneous media [8–12]. Error bounds and convergence studies [13] have shown that these methods exhibit fast convergence rates with increasing orders of expansions. Although this method can deal with large variations of the property, the coupled nature of the resulting equations for the unknown coefficients in the spectral expansion makes the solution of the stochastic problem extremely complex as the number of stochastic dimensions and/or the number of expansion terms increase, the so called *curse of dimensionality*. In fact, computational complexity of the problem increases combinatorially with the number of stochastic dimensions and the number of expansion terms. In addition, it is required to develop a stochastic simulator, which is a non-trivial task especially if the underlying PDEs have complicated nonlinear terms. Therefore, this method is often limited to a small number of inputs (1–10).

There have been recent efforts to couple the fast convergence of the Galerkin methods with the decoupled nature of MC sampling, the so called stochastic collocation method based on sparse grids [14–19]. Hereafter, this method is referred as conventional sparse grid collocation (CSGC) method. This framework represents the stochastic solution as a polynomial approximation. This interpolant is constructed via independent function calls to the deterministic problem at different interpolation points which are selected based on the Smolyak algorithm [20]. This method is also applied to model processes in random heterogeneous media [2,3,21,22]. However, there are several disadvantages. As is well known, the global polynomial interpolation cannot resolve local discontinuity in the stochastic space. Its convergence rate still exhibits a logarithmic dependence on the dimension. For high-dimensional problems, a higher-interpolation level is required to achieve a satisfactory accuracy. However, at the same time, the number of collocation points required increases exponentially for high-dimensional problems (>10) as shown in Fig. 1. Therefore, its computational cost becomes quickly intractable. This method is still limited to a moderate number of random variables (5–15). To this end, Ma and Zabarav [23] extended this methodology to adaptive sparse grid collocation (ASGC). This method utilizes local linear interpolation and uses the magnitude of the hierarchical surplus as an error indicator to detect the non-smooth region in the stochastic space and thus place automatically more points around this region. This approach results in further computational gains and guarantees that a user-defined error threshold is met. In [23], it is shown that the ASGC can successfully resolve stochastic discontinuity problems and solve stochastic elliptic problems up to 100 dimensions when the weights of each dimension are highly anisotropic and thus when the ASGC places more points only along the first few important dimensions. However, it is also shown in the paper that when the importance of each dimension weighs equally, ASGC cannot solve the problem accurately even with a moderate (21) stochastic dimensionality. In this case, the effect of ASGC is nearly the same as of the CSGC and thus the convergence rate deteriorates. As is well known, in realistic random heterogeneous media often we deal with a very small correlation length and

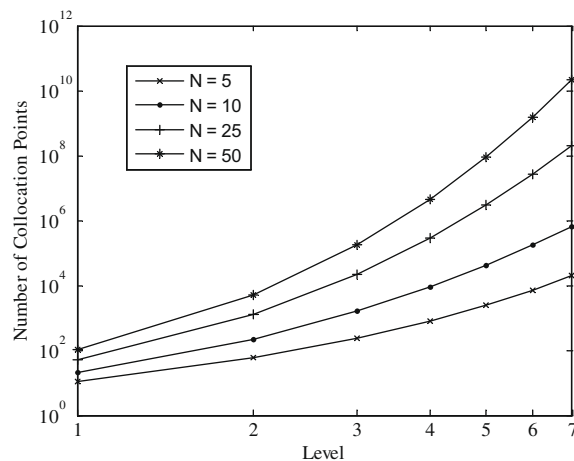


Fig. 1. Number of collocation points versus interpolation level for the conventional sparse grid collocation (CSGC) method.

this results in a rather high-dimensional stochastic space with nearly the same weights along each dimension. In this case, all the previously mentioned stochastic methods are obviously not applicable.

These modeling issues for high-dimensional stochastic problems motivate the use of the so called “High-Dimensional Model Representation” (HDMR) technique. Hereafter, this method is referred as conventional HDMR. It is a general set of quantitative assessment and analysis tools for capturing the high-dimensional relationships between sets of input and output model variables. It was originally developed as a methodology to create an efficient fully equivalent operational model of the original chemical systems [24–29]. It expresses the model output as an additive hierarchical superposition of correlated functions with increasing numbers of input variables, i.e. 1, 2, . . . , up to the total number of input variables. A systematic mapping procedure between the inputs and outputs is prescribed to reveal the hierarchy of correlations among the input variables. At each new level of HDMR, higher-order correlated effects of the input variables are introduced. If these higher-order correlated effects between the input variables have negligible effect upon the output, the HDMR approximation is accurate enough by using only lower-order (usually up to the third-order) component functions. This is the case for most realistic physical systems and is the ansatz that the HDMR is based upon. Depending on the way that one determines the hierarchical component functions in HDMR, there are particularly two types of HDMR: ANOVA-HDMR and CUT-HDMR [24]. ANOVA-HDMR is the same as the analysis of variance (ANOVA) decomposition used in statistics and is useful for measuring the contributions of variance of each component function to the overall variance and therefore for computing the global sensitivity [30]. It involves high-dimensional integration and thus is computationally expensive. On the other hand, the CUT-HDMR expansion is a finite exact representation of the model output in the hyperplane passing through a reference point in the input variable space, which is different from gPC that has infinite terms. It only involves function evaluations at the sample points and is more computationally efficient than ANOVA-HDMR. Therefore, it is our focus in this work.

The model output can be considered as a function taking value over the parameter space supported by the input variables. Therefore, it is also a multivariate function approximation/interpolation method as well as a means to analyze the relevant statistics of the random output, which is the same idea as stochastic collocation method where the solution to the SPDEs is regarded as a stochastic function in the stochastic input space. It is thus straightforward to apply CUT-HDMR in the random space to construct the stochastic input–output mapping. The most important aspect of this method is the capability to find a way to numerically represent each component function of HDMR. In Ref. [31], CUT-HDMR is applied to a transport model to represent the stochastic response and MC analysis is used on the obtained approximation to obtain statistics. However, each CUT-HDMR component function was numerically represented as a low-dimensional look-up table over its variables. To obtain an approximate value, one needs to search and interpolate in the table. In [32,33], CUT-HDMR is derived from a Taylor expansion and is used to find moments of the solution using the so called moment-based quadrature rule in stochastic mechanics. Although the name “dimension reduction method” is used in these papers, it is another form of HDMR. Later, the same author applied this method to fracture and reliability analysis, where component functions are interpolated using tensor product Lagrange polynomials and again MC analysis is used on the obtained approximation to obtain statistics [34,35]. The author in [36] also applied CUT-HDMR to reliability analysis however the interpolant is constructed through moving least squares (MLS) approximation which is only limited up to three dimensions. Most of the above applications approximate each component function on a tensor-product uniform sampling space thus they are very expensive and not very accurate implementations. In addition, all the previous applications are still limited to relatively low-number of stochastic dimensions ( $<12$ ).

In Ref. [37], the authors have applied CUT-HDMR, under the name “Anchored-ANOVA”, to find the mean and variance of the solution using multi-element probabilistic collocation method and integrating the resultant HDMR expansion term by term. In Ref. [38], the authors have applied the same method for the computation of high-dimensional integrals using quadrature schemes with applications to finance. They also developed a dimension-adaptive version of HDMR to find the important component functions and related it with the anisotropic sparse grid method. Motivated by their work, we develop a general framework to combine the strength from both HDMR and ASGC and apply it to uncertainty quantification. We first redefine the way to compute the error indicator in the formulation of ASGC. The use of the magnitude of the hierarchical surplus as the error indicator is too sharp and may result in non-terminating algorithms. The new error indicator incorporates the information from both the basis function and the surplus. This guarantees that the refinement will stop at a sufficient interpolation level. Then HDMR is used to decompose the high-dimensional stochastic problem into several lower-dimensional sub-problems. Each low-dimensional sub-problem is solved by ASGC in a *locally-adaptive* way within only related dimensions. In this way, an efficient low-dimensional stochastic reduced-order model is constructed and any model output in the stochastic space can be interpolated. By using ASGC, the interpolation of component functions is done efficiently by summing the corresponding hierarchical surplus and basis function as compared with that of using a numerical table. Mean and variance can also be obtained analytically through integrating the basis functions without any MC analysis. In addition, the ASGC provides a linear combination of tensor products chosen in such a way that the interpolation error is nearly the same as for full-tensor product (numerical table) in higher dimensions. In practice, HDMR is often truncated into a lower-order representation. However, for a very large stochastic dimension ( $>100$ ), even second-order expansion will have too many component functions. For example, 125,251 component functions are needed for a second-order expansion of a 500-dimensional problem. Therefore, we need to find a way to construct only the important component functions. Motivated by the work in [38], in this paper, we also develop a dimension-adaptive version of HDMR to detect the important component functions. This is defined in two steps: First, the first-order HDMR is constructed and a weight associated with each term is defined to identify the most important dimensions. Then, higher-order components functions are constructed which

consist only of these important dimensions. This method to our knowledge is the first approach which can solve high-dimensional stochastic problems by reducing the dimensions from truncation of HDMR and resolve low-regularity by local adaptivity through ASGC. It is noted here that the adaptivity in our paper is different from that used in [38]. The definition of the error indicator is not the same. The authors in [38] did not identify the important dimensions and thus there is a significant computational overhead in finding the important component functions for high-dimensional problems. It is also noted that in [33,37], the CUT-HDMR is written in an explicit form which is not suitable for adaptive construction. On the other hand, in our paper, a recursive form of an HDMR component function is introduced which is the basis for our adaptive implementation.

This paper is organized as follows: In the next section, the mathematical framework of stochastic PDEs is formulated. In Section 3, the ASGC method for solving PDEs is briefly reviewed. In Section 4, we use HDMR to introduce a new method for solving SPDEs. The numerical examples are given in Section 5. Finally, concluding remarks are provided in Section 6.

## 2. Problem definition

In this section, we follow the notation in [23]. Let us define a complete probability space  $(\Omega, \mathcal{F}, \mathcal{P})$  with sample space  $\Omega$  which corresponds to the outcomes of some experiments,  $\mathcal{F} \subset 2^\Omega$  is the  $\sigma$ -algebra of subsets in  $\Omega$  and  $\mathcal{P} : \mathcal{F} \rightarrow [0, 1]$  is the probability measure. Also, let us define  $D$  as a  $d$ -dimensional bounded domain  $D \subset \mathbb{R}^d$  ( $d = 1, 2, 3$ ) with boundary  $\partial D$ . We are interested in finding a stochastic function  $u : \Omega \times D \rightarrow \mathbb{R}$  such that for  $\mathcal{P}$ -almost everywhere (a.e.)  $\omega \in \Omega$ , the following holds:

$$\mathcal{L}(\mathbf{x}, \omega; u) = \mathbf{g}(\mathbf{x}, \omega), \quad \forall \mathbf{x} \in D, \tag{1}$$

and

$$\mathcal{B}(\mathbf{x}; u) = h(\mathbf{x}), \quad \forall \mathbf{x} \in \partial D, \tag{2}$$

where  $\mathbf{x} = (x_1, \dots, x_d)$  are the coordinates in  $\mathbb{R}^d$ ,  $\mathcal{L}$  is a differential operator, and  $\mathcal{B}$  is a boundary operator. The operators  $\mathcal{L}$  and  $\mathcal{B}$  and the terms  $\mathbf{g}$  and  $h$ , can be assumed random. We assume that the boundary has sufficient regularity and that  $\mathbf{g}$  and  $h$  are properly defined such that the problem in Eqs. (1) and (2) is well-posed for  $\mathcal{P}$ -a.e.  $\omega \in \Omega$ .

### 2.1. The finite-dimensional noise assumption and the Karhunen–Loève expansion

We employ the ‘finite-dimensional noise assumption’ [14] to approximate any second-order stochastic process with a finite-dimensional representation. One such choice is the Karhunen–Loève (K-L) expansion [1]. For example, let the force term  $\mathbf{g}(\mathbf{x}, \omega)$  be a second-order stochastic process, and its covariance function be  $R(\mathbf{x}_1, \mathbf{x}_2)$ , where  $\mathbf{x}_1$  and  $\mathbf{x}_2$  are spatial coordinates. By definition, the covariance function is real, symmetric, and positive definite. All its eigenfunctions are mutually orthonormal and form a complete set spanning the function space to which  $\mathbf{g}(\mathbf{x}, \omega)$  belongs. Then the truncated K-L expansion takes the following form:

$$\mathbf{g}(\mathbf{x}, \omega) = \mathbb{E}[\mathbf{g}(\mathbf{x})] + \sum_{i=1}^N \sqrt{\lambda_i} \phi_i(\mathbf{x}) Y_i(\omega), \tag{3}$$

where  $\{Y_i(\omega)\}_{i=1}^N$  are uncorrelated random variables. If the process is a Gaussian process, then they are standard identically independent  $N(0, 1)$  Gaussian random variables. Also,  $\phi_i(\mathbf{x})$  and  $\lambda_i$  are the eigenfunctions and eigenvalues of the correlation function, respectively. They are the solutions of the following eigenvalue problem:

$$\int_D R(\mathbf{x}_1, \mathbf{x}_2) \phi_i(\mathbf{x}_2) d\mathbf{x}_2 = \lambda_i \phi_i(\mathbf{x}_1). \tag{4}$$

The number of terms needed to approximate a stochastic process depends on the decay rate of the eigenvalues. Generally, a higher-correlation length would lead to a rapid decay of the eigenvalues.

Following a decomposition such as the K-L expansion, the random inputs can be characterized by a set of  $N$  random variables, e.g.

$$\begin{aligned} \mathcal{L}(\mathbf{x}, \omega; u) &= \mathcal{L}(\mathbf{x}, Y_1(\omega), \dots, Y_N(\omega); u), \\ \mathbf{g}(\mathbf{x}, \omega) &= \mathbf{g}(\mathbf{x}, Y_1(\omega), \dots, Y_N(\omega)). \end{aligned} \tag{5}$$

Hence, by using the Doob–Dynkin lemma [39], the solution of Eqs. (1) and (2) can be described by the same set of random variables  $\{Y_i(\omega)\}_{i=1}^N$ , i.e.

$$u(\mathbf{x}, \omega) = u(\mathbf{x}, Y_1(\omega), \dots, Y_N(\omega)). \tag{6}$$

Thus, the use of the spectral expansion guarantees that the finite-dimensional noise assumption is satisfied and effectively reduces the infinite probability space to a  $N$ -dimensional space.

When using the K-L expansion, we here assume that we obtain a set of mutually independent random variables. The issue of non-independent random variables can be resolved by introducing an auxiliary density function [16]. In this work, we

assume that  $\{Y_i(\omega)\}_{i=1}^N$  are independent random variables with probability density functions  $\rho_i, i = 1, \dots, N$ . Let  $\Gamma_i$  be the image of  $Y_i$ . Then

$$\rho(\mathbf{Y}) = \prod_{i=1}^N \rho_i(Y_i), \quad \forall \mathbf{Y} \in \Gamma, \quad (7)$$

is the joint probability density of  $\mathbf{Y} = (Y_1, \dots, Y_N)$  with support

$$\Gamma \equiv \Gamma_1 \times \Gamma_2 \times \dots \times \Gamma_N \in \mathbb{R}^N. \quad (8)$$

Then the problem in Eqs. (1) and (2) can be restated as: Find the stochastic function  $u : \Gamma \times D \rightarrow \mathbb{R}$  such that

$$\mathcal{L}(\mathbf{x}, \mathbf{Y}; u) = g(\mathbf{x}, \mathbf{Y}), \quad (\mathbf{x}, \mathbf{Y}) \in D \times \Gamma, \quad (9)$$

subject to the corresponding boundary conditions

$$\mathcal{B}(\mathbf{x}, \mathbf{Y}; u) = h(\mathbf{x}, \mathbf{Y}), \quad (\mathbf{x}, \mathbf{Y}) \in \partial D \times \Gamma. \quad (10)$$

We assume without loss of generality that the support of the random variables  $Y_i$  is  $\Gamma^i = [0, 1]$  for  $i = 1, \dots, N$  and thus the bounded stochastic space is a  $N$ -hypercube  $\Gamma = [0, 1]^N$ , since any bounded stochastic space can always be mapped to the above hypercube.

The original infinite-dimensional stochastic problem is now restated as a finite-dimensional problem. Then we can apply any stochastic method in the random space and the resulting equations become a set of deterministic equations in the physical space that can be solved by any standard deterministic discretization technique, e.g. the finite element method. The solution to the above SPDE can be regarded as a stochastic function taking real values in the stochastic space  $\Gamma$ . This nature is utilized by the stochastic collocation method which constructs the interpolant of this function in  $\Gamma$  through the Smolyak algorithm. However, this method still suffers from high-dimensionality. In the next few sections, a novel dimension decomposition method is introduced to transform the  $N$ -dimensional problem into several low-dimensional sub-problems.

### 3. Adaptive sparse grid collocation method (ASGC)

In this section, we briefly review the development of the ASGC strategy. For more details, the interested reader is referred to [23].

The basic idea of this method is to have a finite element approximation for the spatial domain and approximate the multi-dimensional stochastic space  $\Gamma$  using interpolating functions on a set of collocation points  $\{\mathbf{Y}_i\}_{i=1}^k \in \Gamma$ . Suppose we can find a finite element approximate solution  $u$  to the deterministic solution of the problem in Eq. (9), we are then interested in constructing an interpolant of  $u$  by using linear combinations of the solutions  $u(\cdot, \mathbf{Y}_i)$ . The interpolation is constructed by using the so called sparse grid interpolation method based on the Smolyak algorithm [20]. In the context of incorporating adaptivity, we have chosen the collocation point based on the Newton-Cotes formulae using equidistant support nodes. The corresponding basis function is the multi-linear basis function constructed from the tensor product of the corresponding one-dimensional functions.

Any function  $f : D \times \Gamma \rightarrow \mathbb{R}$  can now be approximated by the following reduced form:

$$f(\mathbf{x}, \mathbf{Y}) = \sum_{\|\mathbf{i}\| \leq N+q} \sum_{\mathbf{j}} w_{\mathbf{j}}^{\mathbf{i}}(\mathbf{x}) \cdot a_{\mathbf{j}}^{\mathbf{i}}(\mathbf{Y}). \quad (11)$$

where the multi-index  $\mathbf{i} = (i_1, \dots, i_N) \in \mathbb{N}^N$ , the multi-index  $\mathbf{j} = (j_1, \dots, j_N) \in \mathbb{N}^N$  and  $\|\mathbf{i}\| = i_1 + \dots + i_N$ .  $q$  is the sparse grid interpolation level and the summation is over collocation points selected in a hierarchical framework [23]. Here,  $w_{\mathbf{j}}^{\mathbf{i}}$  is the hierarchical surplus, which is just the difference between the function value at the current point and interpolation value from the coarser grid. The hierarchical surplus is a natural candidate for error control and implementation of adaptivity. However, this error indicator is too sharp and may result in a non-terminating algorithm. We will define a new error indicator later.

After obtaining the expression in Eq. (11), it is also easy to extract the statistics [23]. The mean of the random solution can be evaluated as follows:

$$\mathbb{E}[f(\mathbf{x})] = \sum_{\|\mathbf{i}\| \leq N+q} \sum_{\mathbf{j}} w_{\mathbf{j}}^{\mathbf{i}}(\mathbf{x}) \cdot \int_{\Gamma} a_{\mathbf{j}}^{\mathbf{i}}(\mathbf{Y}) d\mathbf{Y}, \quad (12)$$

where the probability density function  $\rho(\mathbf{Y})$  is 1 since the stochastic space is a unit hypercube  $[0, 1]^N$ . As shown in [23], the multi-dimensional integral is simply the product of the 1D integrals which can be computed analytically. Denoting  $\int_{\Gamma} a_{\mathbf{j}}^{\mathbf{i}}(\mathbf{Y}) d\mathbf{Y} = I_{\mathbf{j}}^{\mathbf{i}}$ , we can rewrite Eq. (12) as

$$\mathbb{E}_q[f(\mathbf{x})] = \sum_{\|\mathbf{i}\| \leq N+q} \sum_{\mathbf{j}} w_{\mathbf{j}}^{\mathbf{i}}(\mathbf{x}) \cdot I_{\mathbf{j}}^{\mathbf{i}}. \quad (13)$$

We now define the error indicator as follows:

$$\gamma_j^i = \frac{\|w_j^i(\mathbf{x}) \cdot f_j^i\|_{L_2(D)}}{\|E_{|j|-N-1}f\|_{L_2(D)}}. \tag{14}$$

Here, the  $L_2$  norm is defined in the spatial domain. This error indicator measures the contribution of each term in Eq. (13) to the integration value (mean) relative to the overall integration value computed from the previous interpolation level. In addition to the surpluses, it also incorporates information from the basis functions. This makes the error  $\gamma_j^i$  to decrease to a sufficient small value for a large interpolation level. Therefore, for a reasonable error threshold, this error indicator guarantees that the refinement would stop at a certain interpolation level.

The basic idea of adaptive sparse grid collocation (ASGC) method here is to use the error indicator  $\gamma_j^i$  to detect the smoothness of the solution and refine the hierarchical basis functions  $q_j^i$  whose magnitude of satisfies  $\gamma_j^i \geq \varepsilon$ , where  $\varepsilon$  is a predefined adaptive refinement threshold. If this criterion is satisfied, we simply add the  $2N$  neighbor points of the current point to the sparse grid [23].

#### 4. High-dimensional model representations (HDMR)

In this section, the basic concepts of HDMR are introduced following closely the notation in [24,25,29,38]. For a detailed description of the theory applied to deterministic systems, the interesting reader may refer to [25].

Let  $f(\mathbf{Y}) : \mathbb{R}^N \rightarrow \mathbb{R}$  be a real valued smooth multivariate stochastic function. Here, it is noted that  $f(\mathbf{Y})$  may be also a function of physical coordinate,  $f(\mathbf{Y}, \mathbf{x})$ . From now on, we will omit  $\mathbf{x}$  to simplify the notation. HDMR represents  $f(\mathbf{Y})$  as a finite hierarchical correlated function expansion in terms of the input variables as [24,25,29]

$$f(\mathbf{Y}) = f_0 + \sum_{s=1}^N \sum_{1 \leq i_1 < \dots < i_s} f_{i_1 \dots i_s}(Y_{i_1}, \dots, Y_{i_s}), \tag{15}$$

where the interior sum is over all sets of  $s$  integers  $i_1, \dots, i_s$ , that satisfy  $1 \leq i_1 < i_s \leq N$ . This relation means that

$$f(\mathbf{Y}) = f_0 + \sum_{i=1}^N f_i(Y_i) + \sum_{1 \leq i_1 < i_2 \leq N} f_{i_1 i_2}(Y_{i_1}, Y_{i_2}) + \dots + \sum_{1 \leq i_1 < \dots < i_s \leq N} f_{i_1 \dots i_s}(Y_{i_1}, \dots, Y_{i_s}) + \dots + f_{12 \dots N}(Y_1, \dots, Y_N). \tag{16}$$

Here,  $f_0$  is the zeroth-order component function which is a constant denoting the mean effect. The first-order component function  $f_i(Y_i)$  is a univariate function which represents individual contributions to the output  $f(\mathbf{Y})$ . It is noted that  $f_i(Y_i)$  is general a nonlinear function. The second-order component function  $f_{i_1 i_2}(Y_{i_1}, Y_{i_2})$  is a bivariate function which describes the interactive effects of variables  $Y_{i_1}$  and  $Y_{i_2}$  acting together upon the output  $f(\mathbf{Y})$ . The higher-order terms reflect the cooperative effects of increasing number of input variables acting together to impact  $f$ . The  $s$ -th order component function  $f_{i_1 \dots i_s}(Y_{i_1}, \dots, Y_{i_s})$  is a  $s$ -dimensional function. The last term  $f_{12 \dots N}(Y_1, \dots, Y_N)$  gives any residual dependence of all input variables cooperatively locked together to affect the output  $f(\mathbf{Y})$  [24,25]. Once all the component functions are suitably determined, then the HDMR can be used as a computationally efficient reduced-order model for evaluating the output. This is the same idea as the stochastic collocation method where we also obtain an approximate representation of  $f(\mathbf{Y})$ .

**Remark 1.** The HDMR expansions are based on exploiting the correlation effects of the input variables, which are naturally created by the stochastic input–output mapping, i.e. the SPDE. It is noted that the term “correlation” employed here does not indicate the correlation effects between the input random variables as employed in statistics since in general the random input variables are independent and thus uncorrelated. Instead, it indicates the impact of these input variables upon the system output when acting together.

Eq. (15) is often written in a more compact notation [38] as follows:

$$f(\mathbf{Y}) = \sum_{\mathbf{u} \subseteq \mathcal{D}} f_{\mathbf{u}}(\mathbf{Y}_{\mathbf{u}}), \tag{17}$$

for a given set  $\mathbf{u} \subseteq \mathcal{D}$ , where  $\mathcal{D} := \{1, \dots, N\}$  denotes the set of coordinate indices and  $f_{\emptyset}(\mathbf{Y}_{\emptyset}) = f_0$ . Here,  $\mathbf{Y}_{\mathbf{u}}$  denotes the  $|\mathbf{u}|$ -dimensional vector containing those components of  $\mathbf{Y}$  whose indices belong to the set  $\mathbf{u}$ , where  $|\mathbf{u}|$  is the cardinality of the corresponding set  $\mathbf{u}$ , i.e.  $\mathbf{Y}_{\mathbf{u}} = (Y_i)_{i \in \mathbf{u}}$ . For example, if  $\mathbf{u} = \{1, 3, 5\}$ , then  $|\mathbf{u}| = 3$  and  $f_{\mathbf{u}}(\mathbf{Y}_{\mathbf{u}})$  implies  $f_{135}(Y_1, Y_3, Y_5)$ .

The component functions  $f_{\mathbf{u}}(\mathbf{Y}_{\mathbf{u}})$  can be derived by minimizing the error functional [24,25]:

$$\int_{\Gamma} \left[ f(\mathbf{Y}) - \sum_{\mathbf{u} \subseteq \{0, \dots, s\}} f_{\mathbf{u}}(\mathbf{Y}_{\mathbf{u}}) \right]^2 d\mu(\mathbf{Y}), \tag{18}$$

where  $0 \leq s \leq N$ .

The measure  $d\mu$  determines the particular form of the error functional and of the component functions. The measure  $\mu$  induces the projection operator  $P_{\mathbf{u}} : \Gamma^N \rightarrow \Gamma^{|\mathbf{u}|}$  by [25]

$$P_{\mathbf{u}}f(\mathbf{Y}_{\mathbf{u}}) := \int_{I^{N-|\mathbf{u}|}} f(\mathbf{Y}) d\mu_{\mathcal{D}\setminus\mathbf{u}}(\mathbf{Y}), \tag{19}$$

where  $d\mu_{\mathcal{D}\setminus\mathbf{u}}(\mathbf{Y}) := \prod_{i \in \mathcal{D}, i \notin \mathbf{u}} d\mu_i(Y_i)$ .

Therefore, the  $2^N$  terms  $f_{\mathbf{u}}$  can be recursively defined by [24]

$$f_{\mathbf{u}}(\mathbf{Y}_{\mathbf{u}}) := P_{\mathbf{u}}f(\mathbf{Y}_{\mathbf{u}}) - \sum_{\mathbf{v} \subset \mathbf{u}} f_{\mathbf{v}}(\mathbf{Y}_{\mathbf{v}}), \tag{20}$$

and can also be given explicitly by [40]

$$f_{\mathbf{u}}(\mathbf{Y}_{\mathbf{u}}) := \sum_{\mathbf{v} \subset \mathbf{u}} (-1)^{|\mathbf{u}|-|\mathbf{v}|} P_{\mathbf{v}}f(\mathbf{Y}_{\mathbf{v}}). \tag{21}$$

This formulation is particularly useful to combine with ASGC as will be discussed later. The component functions are orthogonal with respect to the inner product induced by the measure  $\mu$ ,

$$\int_{I^N} f_{\mathbf{u}}(\mathbf{Y}_{\mathbf{u}}) f_{\mathbf{v}}(\mathbf{Y}_{\mathbf{v}}) d\mu(\mathbf{Y}) = 0, \quad \text{for } \mathbf{u} \neq \mathbf{v}, \tag{22}$$

and thus the resulting decomposition Eq. (17) is unique for a fixed measure  $\mu$ . In the next sections, we will present two particularly useful decompositions.

#### 4.1. ANOVA-HDMR

In this case, the measure  $\mu$  is taken as the ordinary Lebesgue measure  $d\mu(\mathbf{Y}) = d(\mathbf{Y}) = \prod_{i=1}^N dY_i$ . With this choice, the actions of the projection operators in the ANOVA-HDMR are given by

$$P_{\mathbf{u}}f(\mathbf{Y}_{\mathbf{u}}) := \int_{I^{N-|\mathbf{u}|}} f(\mathbf{Y}) d\mathbf{Y}_{\mathcal{D}\setminus\mathbf{u}}. \tag{23}$$

More specifically, the first few terms are

$$\begin{aligned} f_0 &= \int_{I^N} f(\mathbf{Y}) d\mathbf{Y}, \quad f_i(Y_i) = \int_{I^{N-1}} f(\mathbf{Y}) \prod_{j \neq i} dY_j - f_0 \\ f_{ij}(Y_i, Y_j) &= \int_{I^{N-2}} f(\mathbf{Y}) \prod_{k \neq i, j} dY_k - f_i(Y_i) - f_j(Y_j) - f_0, \dots \end{aligned} \tag{24}$$

This decomposition is the same as the well-known analysis of variance (ANOVA) decomposition used in statistics. A significant drawback of ANOVA-HDMR is the need to compute the high-dimensional integrals. Even the zeroth-order component function requires a full-dimensional integration in the space. To circumvent this difficulty, a computationally more efficient CUT-HDMR expansion will be introduced in the following section for the stochastic model representation which is the focus of this paper.

#### 4.2. CUT-HDMR

In this work, the CUT-HDMR is adopted to construct the response surface of the stochastic solution. With this method, the measure  $\mu$  is chosen as the Dirac measure located at a reference point  $\bar{\mathbf{Y}} = (\bar{Y}_1, \bar{Y}_2, \dots, \bar{Y}_N)$ , i.e.  $d\mu(\mathbf{Y}) = \prod_{i=1}^N \delta(Y_i - \bar{Y}_i) dY_i$ . With this choice, the projections Eq. (19) become

$$P_{\mathbf{u}}f(\mathbf{Y}_{\mathbf{u}}) := f(\mathbf{Y})|_{\mathbf{Y}=\bar{\mathbf{Y}}_{\setminus\mathbf{u}}}, \tag{25}$$

where the notation  $\mathbf{Y} = \bar{\mathbf{Y}} \setminus \mathbf{Y}_{\mathbf{u}}$  means that the components of  $\mathbf{Y}$  other than those indices that belong to the set  $\mathbf{u}$  are set equal to those of the reference point. Eq. (25) defines a  $|\mathbf{u}|$ -dimensional function where the unknown variables are those dimensions whose indices belong to  $\mathbf{u}$ . The component functions of CUT-HDMR are explicitly given as follows [24]:

$$\begin{aligned} f_0 &= f(\bar{\mathbf{Y}}), \quad f_i(Y_i) = f(\mathbf{Y})|_{\mathbf{Y}=\bar{\mathbf{Y}}_{\setminus Y_i}} - f_0 \\ f_{ij}(Y_i, Y_j) &= f(\mathbf{Y})|_{\mathbf{Y}=\bar{\mathbf{Y}}_{\setminus (Y_i, Y_j)}} - f_i(Y_i) - f_j(Y_j) - f_0, \dots \end{aligned} \tag{26}$$

It is argued in [24,25] that quite often in typical deterministic physical systems the correlation effects of the higher-order terms among the input variables for their action upon the output are weak. Tests on several examples from [24,25] indicate that only the low-order correlations have a significant impact on the output and thus the few lower-order terms (usually up to third-order) are often sufficient to represent the model to a desired accuracy. The extent of high-order variable cooperativity depends on the choice of input variables [25]. However, the exact factors which determine the correlation effect in stochastic space are unclear and this will be one of the focus points of this paper.

It is also interesting to note that the CUT-HDMR can be derived from a Taylor expansion at the reference point [33]:

$$f(\mathbf{Y}) = f(\bar{\mathbf{Y}}) + \sum_{j=1}^{\infty} \frac{1}{j!} \sum_{i=1}^N \frac{\partial^j f}{\partial Y_i^j}(\bar{\mathbf{Y}})(Y_i - \bar{Y}_i)^j + \sum_{j_1, j_2 > 0}^{\infty} \frac{1}{j_1! j_2!} \sum_{i_1 < i_2} \frac{\partial^{j_1+j_2} f}{\partial Y_{i_1}^{j_1} \partial Y_{i_2}^{j_2}}(\bar{\mathbf{Y}})(Y_{i_1} - \bar{Y}_{i_1})^{j_1} (Y_{i_2} - \bar{Y}_{i_2})^{j_2} + \dots \tag{27}$$

The infinite number of terms in the Taylor series are partitioned into finite number of groups with each group corresponding to one CUT-HDMR component function. For example, the first-order component function  $f_i(Y_i)$  is the sum of all the Taylor series terms which contain and only contain variable  $Y_i$  and so on [28]. Any truncated HDMR expansion should provide high-order accuracy than a truncated Taylor series of the same order.

#### 4.2.1. Choice of the reference point

The convergence property of HDMR is rather sensitive to the choice of the reference point. It is argued in [24] that the reference point can be chosen arbitrarily provided the HDMR expansion is converged. Later, it is pointed out in [29,41] that in some cases the choice of the reference point is important in order to obtain a good approximation for a fixed-order HDMR and a careless choice may lead to an unacceptable approximation error.

We would like to choose a suitable point such that the error of a fixed-order HDMR approximation is as small as possible and the HDMR expansion order is as low as possible. The authors in [29,41] proved that a good reference point should satisfy:

$$\min_{\mathbf{Y} \in \mathcal{I}} |f(\bar{\mathbf{Y}}) - \mathbb{E}[f(\mathbf{Y})]|. \tag{28}$$

However, the mean of the output is not known *a priori*. To this end, they proposed to sample a moderate number of random inputs and compute the mean of the sample outputs. Then the reference point is chosen as the one among the samples whose output is the closest to the above mean value [29,41]. It is obvious that this method will be quite expensive if it is used in our problem.

According to the Taylor expansion Eq. (27), if we choose the reference point as the mean of the input random vector, then the expectation of the output is close to the function value at the mean vector since the coefficients associated with higher-order terms in the Taylor series are usually much smaller than lower-order terms. It has been shown that in many stochastic mechanics problems [33], a second-order HDMR expansion usually leads to a satisfactory approximation within a desired accuracy if the reference point is chosen as the mean vector. Therefore, unless otherwise stated, we always choose the mean of the random input vector as the reference point in this paper.

### 4.3. Integrating HDMR and ASGC

Although ASGC depends less on dimensionality than the gPC method, it still suffers with increasing number of dimensions [23]. Therefore, for problems with high stochastic dimensionality, to obtain accurate results one needs to use a higher-interpolation level. However, the number of needed points will grow quickly as shown in Fig. 1. Integrating HDMR and ASGC is a way to address and overcome this difficulty.

Within the framework of CUT-HDMR, let us rewrite Eqs. (17) and (21) as

$$f(\mathbf{Y}) = \sum_{\mathbf{u} \subseteq \mathcal{D}} f_{\mathbf{u}}(\mathbf{Y}_{\mathbf{u}}) = \sum_{\mathbf{u} \subseteq \mathcal{D}} \sum_{\mathbf{v} \subseteq \mathbf{u}} (-1)^{|\mathbf{u}| - |\mathbf{v}|} f(\mathbf{Y}_{\mathbf{v}})_{\mathbf{Y} = \bar{\mathbf{Y}}_{\mathbf{v}}}, \tag{29}$$

where we define  $f(\mathbf{Y}_{\emptyset}) = f(\bar{\mathbf{Y}})$ . Therefore, the  $N$ -dimensional stochastic problem is transformed to several lower-order  $|\mathbf{v}|$ -dimensional problems  $f(\mathbf{Y}_{\mathbf{v}})_{\mathbf{Y} = \bar{\mathbf{Y}}_{\mathbf{v}}}$  which can be easily solved by the ASGC as introduced in the last section:

$$f(\mathbf{Y}) = \sum_{\mathbf{u} \subseteq \mathcal{D}} \sum_{\mathbf{v} \subseteq \mathbf{u}} (-1)^{|\mathbf{u}| - |\mathbf{v}|} \sum_{\|\mathbf{i}\| \leq N+q} \sum_{\mathbf{j}} w_{\mathbf{v}}^{\mathbf{i}, \mathbf{j}}(\mathbf{x}) \cdot a_{\mathbf{j}}^{\mathbf{i}}(\mathbf{Y}_{\mathbf{v}}), \tag{30}$$

where  $\|\mathbf{i}\| = i_1 + \dots + i_{|\mathbf{v}|}$ ,  $w_{\mathbf{v}}^{\mathbf{i}, \mathbf{j}}(\mathbf{x})$  are the hierarchical surpluses for different sub-problems indexed by  $\mathbf{v}$  and  $a_{\mathbf{j}}^{\mathbf{i}}(\mathbf{Y}_{\mathbf{v}})$  is only a function of the coordinates which belong to the set  $\mathbf{v}$ . It is noted that the interpolation level  $q$  may be different for each sub-problem according to their regularity along the particular dimensions which is controlled by the error threshold  $\varepsilon$ . In this work,  $\varepsilon$  is the same for all sub-problems.

Interpolation is done quickly here (with no need to search any tables) through simple weighted sum of the basis functions and the corresponding hierarchical surpluses. In addition, it is also easy to extract statistics as introduced in Section 3 by integrating directly the interpolating basis functions. Let us denote

$$J_{\mathbf{u}} = \sum_{\mathbf{v} \subseteq \mathbf{u}} (-1)^{|\mathbf{u}| - |\mathbf{v}|} \sum_{\|\mathbf{i}\| \leq N+q} \sum_{\mathbf{j}} w_{\mathbf{v}}^{\mathbf{i}, \mathbf{j}}(\mathbf{x}) \cdot I_{\mathbf{j}}^{\mathbf{i}}, \tag{31}$$

as the mean of the component function  $f_{\mathbf{u}}$ . Then the mean of the HDMR expansion is simply  $\mathbb{E}[f(\mathbf{Y})] = \sum_{\mathbf{u} \subseteq \mathcal{D}} J_{\mathbf{u}}$ . To obtain the variance of the solution, we can similarly construct an approximation for  $u^2$  and use the formula  $\text{Var}[u(\mathbf{x})] = \mathbb{E}[u^2(\mathbf{x})] - (\mathbb{E}[u(\mathbf{x})])^2$ .

**Remark 2.** It is also possible to use the Smolyak quadrature rule directly to integrate the CUT-HDMR in order to obtain the mean and the variance [37,38]. However, the method introduced here is much better since it provides a function approximation to the output that can be used as a stochastic reduced-order model [42] with local adaptivity built in its representation.

4.4. The effective dimension of a multivariate stochastic function

Related to HDMR expansions is the concept of the effective dimension of a multivariate function [38,40]. In Ref. [38], the authors have discussed it in the case of integration. Here, we extend this concept to a multivariate stochastic function. Let  $\hat{f} := \sum_{\mathbf{u} \subseteq \mathcal{D}} |\mathbf{J}_{\mathbf{u}}|$  be the sum of all contributions to the mean value, where  $|\mathbf{J}_{\mathbf{u}}| = |\int f_{\mathbf{u}} d\mathbf{Y}_{\mathbf{u}}| \leq \|f_{\mathbf{u}}\|_{L_1}$  [38]. Then, for the proportion  $\alpha \in (0, 1]$ , the *truncation dimension* is defined as the smallest integer  $N_t$ , such that

$$\sum_{\mathbf{u} \subseteq \{1, \dots, N_t\}} |\mathbf{J}_{\mathbf{u}}| \geq \alpha \hat{f}, \tag{32}$$

whereas, the *superposition dimension* is defined as the smallest integer  $N_s$ , such that

$$\sum_{|\mathbf{u}| \leq N_s} |\mathbf{J}_{\mathbf{u}}| \geq \alpha \hat{f}. \tag{33}$$

The superposition dimension is also called the *order* of the HDMR expansion. The effective dimensions in the case of interpolation cannot be defined in a unique manner and their definition is part of the algorithmic approach used.

With the definition of effective dimensions, we can thus truncate the expansion in Eq. (17). In other words, we take only a subset  $\mathcal{S}$  of all indices  $\mathbf{u} \subseteq \mathcal{D}$ . Here, we assume that the set  $\mathcal{S}$  satisfies the following admissibility condition:

$$\mathbf{u} \in \mathcal{S} \quad \text{and} \quad \mathbf{v} \subset \mathbf{u} \Rightarrow \mathbf{v} \in \mathcal{S}. \tag{34}$$

This is to guarantee that all the terms can be calculated according to Eq. (21). For example, the set of indices based on the superposition dimension can be defined as  $\mathcal{S}_{N_s} := \{\mathbf{u} \subseteq \mathcal{D} : |\mathbf{u}| \leq N_s\}$  and the set of indices based on the truncation dimension can be defined as  $\mathcal{S}_{N_t} := \{\mathbf{u} \subseteq \{1, \dots, N_t\}\}$ .

Therefore, from Section 4.3, we can define an interpolation formula  $\mathcal{A}_{\mathcal{S}}f$  for the approximation of  $f$  which is given by

$$\mathcal{A}_{\mathcal{S}}f := \sum_{\mathbf{u} \in \mathcal{S}} \mathcal{A}(f_{\mathbf{u}}). \tag{35}$$

Here  $\mathcal{A}(f_{\mathbf{u}})$  is the sparse grid interpolant of the component function  $f_{\mathbf{u}}$  and  $\mathcal{A}_{\mathcal{S}}f$  is the interpolant of the function  $f$  using the proposed method with the index set  $\mathcal{S}$ . It is common to refer to the terms  $\{f_{\mathbf{u}} : |\mathbf{u}| = l\}$  collectively as the “order- $l$  terms”. Then the expansion order,  $p$ , for the decomposition Eq. (35) is defined as the maximum of  $l$ . Note that the number of collocation points in this expansion is defined as the sum of the number of points for each sub-problem from Eq. (30), i.e.  $M = \sum_{\mathbf{u} \in \mathcal{S}} M_{\mathbf{u}}$ .

Now, let us consider the approximation error of the truncated HDMR expansion with ASGC used for the component functions in Eq. (35). To this end, we fix  $\alpha \in (0, 1]$  and assume that  $N_s$  and  $N_t$ , the corresponding superposition and truncation dimensions, are known. We define the index set  $\mathcal{S}_{N_t, N_s} := \{\mathbf{u} \subseteq \{1, \dots, N_t\}, |\mathbf{u}| \leq N_s\}$ . We can state the following theorem:

**Theorem 1.** Let  $\mathcal{S} = \mathcal{S}_{N_t, N_s}$ , and let  $\mathcal{A}$  be the ASGC interpolant with the same error threshold  $\varepsilon$  for all the sub-problems. Then:

$$|f - \mathcal{A}_{\mathcal{S}}f| \leq c(N_s, N_t)\varepsilon + \varepsilon_t, \tag{36}$$

for all  $f \in F_N$ , where  $F_N := \{f : [0, 1]^N \rightarrow \mathbb{R}, D^{|\mathbf{m}|}f \text{ continuous}, m_i \leq 2, \forall i\}$ . Here, the constant  $c(N_t, N_s)$  depends on the effective dimensions but does not depend on the nominal dimension  $N$ .  $\varepsilon_t$  is the truncation error of Eq. (35) according to the definition of effective dimensions.

**Proof.** The proof of this theorem is similar to that of Theorem 3.3 in [38]. We start with

$$|f - \mathcal{A}_{\mathcal{S}}f| \leq |f - f_{\mathcal{S}}| + |f_{\mathcal{S}} - \mathcal{A}_{\mathcal{S}}f|, \tag{37}$$

where  $f_{\mathcal{S}} := \sum_{\mathbf{u} \in \mathcal{S}_{N_t, N_s}} f_{\mathbf{u}}(\mathbf{Y}_{\mathbf{u}})$ . The first term on the right hand side is the truncation error and the second term is the interpolation error. According to the definition of effective dimensions, with increasing  $\alpha \in (0, 1]$ , the approximation approaches the true value. Therefore, for a fixed  $\alpha$ , we can denote the truncation error as  $|f - f_{\mathcal{S}}| = \varepsilon_t$ . From Eq. (21), we have the expression

$$f_{\mathbf{u}} - \mathcal{A}(f_{\mathbf{u}}) = \sum_{\mathbf{v} \subset \mathbf{u}} (-1)^{|\mathbf{u}| - |\mathbf{v}|} (P_{\mathbf{v}}f - \mathcal{A}(P_{\mathbf{v}}f)). \tag{38}$$

According to the ASGC algorithm, it is known that the approximation error is controlled by the error threshold  $\varepsilon$ . Since we choose the same  $\varepsilon$  for each sub-problem, we have  $|P_{\mathbf{v}}f - \mathcal{A}(P_{\mathbf{v}}f)| \leq \varepsilon$  [23].

Therefore, we have

$$|f_{\mathcal{S}} - \mathcal{A}_{\mathcal{S}}(f)| \leq \sum_{\mathbf{u} \in \mathcal{S}} |f_{\mathbf{u}} - \mathcal{A}(f_{\mathbf{u}})| \leq \sum_{\mathbf{u} \in \mathcal{S}} \sum_{\mathbf{v} \subset \mathbf{u}} |P_{\mathbf{v}}f - \mathcal{A}(P_{\mathbf{v}}f)| \leq \sum_{\mathbf{u} \in \mathcal{S}} \sum_{\mathbf{v} \subset \mathbf{u}} \varepsilon = \sum_{k=1}^{N_t} \binom{N_t}{k} \sum_{j=1}^k \binom{k}{j} \varepsilon \leq c(N_t, N_s)\varepsilon, \tag{39}$$

with the constant  $c(N_t, N_s)$  given as [38]

$$c(N_t, N_s) := \sum_{k=1}^{N_s} \binom{N_t}{k} \sum_{j=1}^k \binom{k}{j} \leq \sum_{k=1}^{N_s} \binom{N_t}{k} 2^k \leq 2^{N_s+1} N_t^{N_s},$$

which completes the proof. □

Therefore, it is expected that the expansion Eq. (35) converges to the true value with decreasing error threshold  $\varepsilon$  and increasing number of component functions.

#### 4.5. Adaptive HDMR

In practice, the effective dimensions are not known *a priori*. In order to find the effective dimensions, one needs to compute all  $2^N$  component functions. They were originally defined for the representation of pure mathematical functions [29,38]. However, in our case, calculating effective dimensions is not practical since we need to solve PDEs and thus the computational cost is much higher than that for function evaluation. Note that the total number of component functions for a  $l$ -th order expansion is  $\sum_{i=0}^l \frac{N!}{i!(N-i)!}$ , which increases quickly with the number of dimensions. Therefore, in this section, we would like to develop an adaptive version of HDMR for automatically and simultaneously detecting the truncation and superposition dimensions.

We here assume each component function  $f_{\mathbf{u}}$  is associated with a weight  $\eta_{\mathbf{u}} \geq 0$ , which describes the contribution of the term  $f_{\mathbf{u}}$  to the HDMR. Using this information, we then want to automatically determine the optimal index set  $\mathcal{S}$ , which consists of two steps.

At first, we try to find the important dimensions, i.e. the truncation dimension. To this end, we always construct the zeroth- and first-order HDMR expansion where the computational cost is affordable even for very high-dimensions. In this case, the weight is defined as:

$$\eta_i = \frac{\|J_{(i)}\|_{L_2(D)}}{\|f_0(\bar{\mathbf{Y}})\|_{L_2(D)}}, \tag{40}$$

where  $J_{(i)} = \int f_i(Y_i) dY_i$  follows the definition in Eq. (31) and the  $L_2$  norm is defined in the spatial domain when the output is a function of spatial coordinates. Each first-order component function is only a one-dimensional function which measures the impact on the output when each dimension is acting independently. According to Eqs. (26) and (40), this weight can be considered as a measurement of the sensitivity of the output when only the  $i$ th-dimension is the input. Then we define the important dimensions as those whose weights are larger than a predefined error threshold  $\theta_1$ . Now, the set  $\mathcal{D}$  in Eq. (29) only contains these important dimensions instead of all the dimensions. For example, if the important dimensions are 1, 3 and 5, then only the higher-order terms {13}, {15}, {35} and {135} are considered. It is noted that the important dimensions depend on the choice of  $\theta_1$ . With decreasing  $\theta_1$ , more dimensions become important and therefore more terms need to be included in the HDMR.

The reason for defining the weight in Eq. (40) is as follows. HDMR is aimed to reveal the correlation effects among the input variables as reflected upon the output. The correlation effect is large if the change of the random input within its range will lead to a significant change on the output. According to the definition of first-order component function,  $f_i(Y_i) = f(\mathbf{Y})|_{\mathbf{Y}=\bar{\mathbf{Y}}, Y_i} - f_0$ ,  $f_i(Y_i)$  measures the difference between the function value with only input arising from one dimension acting independently and the function value at the reference point. It contains the information about the impact upon the output from this particular dimension. Therefore, if the weight is defined as in Eq. (40), it clearly gives us information on the impact that this dimension has when is acting alone upon the output. Only those dimensions which have significant impact on the output are considered as important. Then it is straightforward to argue that if two dimensions are important, there is a possibility that the impact upon the output is still significant if these two dimensions act together. Therefore, we need to consider all the component functions of only these important dimensions. It is noted that a similar definition is also proposed in [38] and is proved to be effective.

However, not all the possible terms are computed. Instead, we adaptively construct higher-order component functions increasingly from lower-order to higher-order in order to reduce the computational cost in the following way. For each computed higher-order term  $f_{\mathbf{u}}$ ,  $|\mathbf{u}| \geq 2$ , a weight is also defined as

$$\eta_{\mathbf{u}} = \frac{\|J_{\mathbf{u}}\|_{L_2(D)}}{\left\| \sum_{\mathbf{v} \in \mathcal{S}, |\mathbf{v}| \leq |\mathbf{u}|-1} J_{\mathbf{v}} \right\|_{L_2(D)}}. \tag{41}$$

It measures the relative importance with respect to the sum of current integral value which has already been computed in set  $\mathcal{S}$  from the previous order. Similarly, the important component functions are defined as those whose weights are larger than the predefined error threshold  $\theta_1$ . We put all the important dimensions and higher-order terms into a set  $\mathcal{T}$ , which is called the important set. When adaptively constructing HDMR for each new order, we only calculate the term  $f_{\mathbf{u}}$  whose indices satisfy the admissibility relation Eq. (34),

$$\mathbf{u} \in \mathcal{D} \text{ and } \mathbf{v} \subset \mathbf{u} \Rightarrow \mathbf{v} \in \mathcal{T}. \quad (42)$$

In other words, among all the possible indices, we only want to find the terms which can be computed using the previous known important component functions via Eq. (20). In this way, we find those terms which may have significant contribution to the overall expansion while ignoring other trivial terms thus reducing the computational cost for high-dimensional problems.

Let us denote the order of expansion as  $p$ . Furthermore, we also define a relative error  $\rho$  of the integral value between two consecutive expansion orders  $p$  and  $p-1$  as

$$\rho = \frac{\left\| \sum_{|\mathbf{u}| \leq p} J_{\mathbf{u}} - \sum_{|\mathbf{u}| \leq p-1} J_{\mathbf{u}} \right\|_{L_2(D)}}{\left\| \sum_{|\mathbf{u}| \leq p-1} J_{\mathbf{u}} \right\|_{L_2(D)}}. \quad (43)$$

If  $\rho$  is smaller than another predefined error threshold  $\theta_2$ , we consider that the HDMR has converged and the construction stops.

The above procedure is detailed in Algorithm 1.

**Algorithm 1.** Adaptive construction of the index set  $\mathcal{S}$ .

**Initialize:** Let  $\mathcal{S} = \{\emptyset\}$ ,  $\mathcal{R} = \{\emptyset\}$  and  $\mathcal{T} = \{\emptyset\}$ . Set  $p = 1$ .

Construct the zeroth and first-order component functions:

- Solve each sub-problem using the ASGC method with error threshold  $\varepsilon$  and add all the indices to  $\mathcal{S}$ .
- Compute the weights of each first-order term according to Eq. (40). Add those dimensions which satisfy  $\eta \geq \theta_1$  to set  $\mathcal{T}$ .

**repeat**

- $p \leftarrow p + 1$ . Construct the set  $\mathcal{R}$  whose indices satisfy the admissibility relation Eq. (42) for  $|\mathbf{u}| = p$ .
- If  $\mathcal{R} \neq \{\emptyset\}$ , for each index  $\mathbf{u} \in \mathcal{R}$ , solve the corresponding sub-problem using ASGC with error threshold  $\varepsilon$  and add all the indices to  $\mathcal{S}$ .
- Compute the weight of component functions according to Eq. (41). Add those indices which satisfy  $\eta \geq \theta_1$  to set  $\mathcal{T}$  and clear set  $\mathcal{R}$ .
- Compute the relative error  $\rho$  according to Eq. (43).

**until**  $\mathcal{R} = \{\emptyset\}$  or  $\rho < \theta_2$ ;

It is noted here that we add all the computed indices to set  $\mathcal{S}$  even if their weight is below the threshold  $\theta_1$  in order to further improve the accuracy since we have already paid the cost to compute them. This is similar idea to that used in the ASGC algorithm [23].

Before closing this section, we want to comment again on the definition of the weights in Eqs. (40) and (41). As discussed before, these weights provide information on the contribution of each component function to the overall expansion. In addition, the weights from the first-order expansion also provide us information on the important dimensions. An important dimension here is defined in a relative sense, which means that its impact upon the output is more significant than that of others. Here, we provide a guideline to select  $\theta_1$ . Since the expansion of each order only depends on the previous order, we can first only construct the first-order expansion. Then we can sort all dimensions in a descending order according to the value of  $\eta_i$ . Finally, the value of  $\theta_1$  is chosen such that only a certain portion of the dimensions are considered important. If all the weights are the same, we have to include all the dimensions. Although we do not have the situation in the numerical examples considered here, there is a possibility that  $\|f_0(\bar{\mathbf{Y}})\|_{L_2} = 0$ . In this case, one can simply define  $\eta_i = \|J_{\{i\}}\|_{L_2}$ .

## 5. Numerical examples

In this section, two sets of numerical examples are considered to illustrate the proposed HDMR technique. In the investigations below we consider both *adaptive HDMR* and *conventional HDMR* where the adaptivity here refers only to the truncation of the expansion. In all examples, the ASGC method is used for the calculation of the component functions. The ASGC method used alone refers to the adaptive sparse grid collocation in [23] applied directly (without HDMR expansion) to the interpolation of the original function of interest or to the solution of the SPDE. Similarly, CSGC refers to the conventional sparse grid interpolation without adaptivity applied to the original function or solution of the SPDE. The first set of examples involves elementary mathematical functions while the second set involves stochastic fluid mechanics problems. Whenever possible, comparisons with alternative methods are provided to evaluate the accuracy, computational efficiency, and convergence of the proposed method. In the following examples, unless otherwise specified,  $\theta_2$  is fixed at  $10^{-4}$ .

### 5.1. Example set I – mathematical functions

It is noted that according to the right hand side of HDMR Eq. (15), if the function has an additive structure, then HDMR is exact, e.g. when  $f(\mathbf{Y})$  can be additively decomposed into functions  $f_i(Y_i)$  of single variables, then the first-order expansion is enough to exactly represent the original function. On the other hand, if a multiplicative nature of the function is dominant

then all components of HDMR may be needed to obtain an accurate result. However, if HDMR requires all  $2^N$  components to obtain a desired accuracy, the method becomes very expensive. This example is designed to investigate how function structure and input variability affect the accuracy of the proposed method.

5.2. Example 1

Let us first consider the following simple function which has an additive structure in  $[0, 1]^N$ :

$$f(\mathbf{Y}) = \sum_{i=1}^N Y_i^2. \tag{44}$$

where  $Y_i$  are uniform random variables with range  $[0,1]$ . Here, we take  $N = 10$  and a third-order conventional HDMR expansion with  $\varepsilon = 10^{-4}$ . After constructing the HDMR, we generate 100 random points and compare the interpolating results of HDMR with the exact value. The normalized  $L_2$  error is defined as

$$\epsilon_{L_2} = \frac{\sqrt{\sum_{i=1}^{100} (f_{\text{HDMR}}(\mathbf{Y}_i) - f_{\text{exact}}(\mathbf{Y}_i))^2}}{\sqrt{\sum_{i=1}^{100} f_{\text{exact}}(\mathbf{Y}_i)^2}} \tag{45}$$

The result is shown in Table 1. As expected, only first-order HDMR is enough to represent the function exactly. Increasing the expansion order does not improve the accuracy.

We compare next the convergence rate of first-order HDMR with other methods, which is shown in Fig. 2. Using HDMR, the number of points required to achieve a certain level of accuracy is much less than that using other methods. The number of points for CSGC at level 6 is 171,425, when going to the next level, the number increases to 652,065. The number of points using ASGC alone is 12621. It is also interesting to note that the convergence rate of HDMR is the same as for ASGC, which shows that the error of HDMR is also controlled by  $\varepsilon$ . To further verify the results numerically, we compare the maximum error with respect to different  $\varepsilon$  for HDMR and ASGC, respectively, in Table 2. As expected the error threshold  $\varepsilon$  also controls the error of a converged HDMR. This can be partially explained as follows. From Eq. (36), the error of HDMR consists of two parts: truncation error of HDMR and interpolation error of ASGC in the component function calculation. When HDMR has converged, the error is only determined by the interpolation error of each low-dimensional component function using ASGC which is also  $\varepsilon$ , and recall that HDMR is a linear combination of all the low-dimensional functions. Therefore the error is approximately  $C\varepsilon$ , where  $C$  is a constant. This case suggests that a lower-order converged HDMR is a good substitute of ASGC with much less needed number of collocation points.

5.3. Example 2

Next we consider the function “product peak” in  $[0, 1]^N$  from GENZ test package [43] which has multiplicative nature:

$$f(\mathbf{Y}) = \prod_{i=1}^N (c_i^{-2} + (Y_i - w_i)^2)^{-1}, \tag{46}$$

where  $c_i$  and  $w_i$  are constants and  $N = 10$ .  $Y_i$  are uniform random variables with range  $[0,1]$ . The interpolation error is defined the same as before. The integration (mean) value of this function is defined as  $I = \int_{[1,0]^{10}} f(\mathbf{Y}) d\mathbf{Y}$ . The relative integration error is defined as  $\frac{|I_{\text{num}} - I_{\text{exact}}|}{|I_{\text{exact}}|}$  where the exact value is available analytically.

We first examine the convergence of the HDMR with different expansion orders while fixing  $\varepsilon = 10^{-6}$ , which is shown in Fig. 3. Unlike the previous example, we now need all the terms in the HDMR expansion to obtain the exact result due to the multiplicative structure of the function. However, it is seen that the interpolation error decreases quickly with increasing expansion order. At least a fifth-order expansion is needed to achieve accuracy of  $\mathcal{O}(10^{-3})$  in this case. It is also interesting to note that HDMR converges faster for integration. Since the integration (mean) value is a statistical measure, it possibly suggests that the convergence rate depends more on the statistics of the input than the structure of the function itself. We will further investigate this in the next example.

In Table 3, we also report the convergence of the ASGC used in the calculation of the component functions for a fixed HDMR expansion order. In the combination of each order and  $\varepsilon$ , the first column is the  $L_2$  interpolation error and the second

**Table 1**  
Interpolation of the function in Eq. (44) using HDMR of different orders with interpolation error threshold  $\varepsilon = 10^{-4}$ .

$N = 10$	# Points	$L_2$ Error
1st order HDMR	1291	$1.3027 \times 10^{-4}$
2nd order HDMR	33,016	$1.3027 \times 10^{-4}$
3rd order HDMR	340,336	$1.3027 \times 10^{-4}$

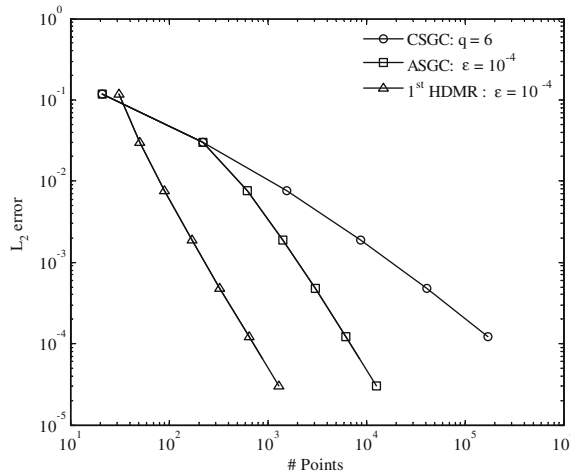


Fig. 2.  $L_2$  interpolation error versus number of points for the function in Eq. (44).

Table 2

Maximum error using first-order HDMR and ASGC with various  $\epsilon$ .

$N = 10$	HDMR		ASGC	
	# Points	MaxError	# Points	MaxError
$\epsilon = 10^{-1}$	51	$1.3887 \times 10^{-1}$	221	$1.3887 \times 10^{-1}$
$\epsilon = 10^{-2}$	171	$8.3629 \times 10^{-3}$	1421	$8.3629 \times 10^{-3}$
$\epsilon = 10^{-3}$	331	$2.1349 \times 10^{-3}$	3021	$2.1349 \times 10^{-3}$
$\epsilon = 10^{-4}$	1291	$1.3027 \times 10^{-4}$	12,621	$1.3027 \times 10^{-4}$
$\epsilon = 10^{-5}$	5131	$8.3142 \times 10^{-6}$	51,021	$8.3142 \times 10^{-6}$

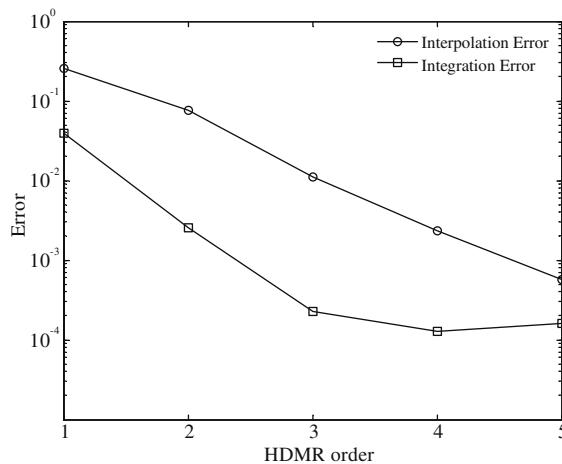


Fig. 3. Convergence of HDMR for the function in Eq. (46) with different orders.

Table 3

Relative errors for various HDMR expansion order and error threshold. In each combination, the first column is the  $L_2$  interpolation error and the second is the relative mean error.

Order	$\epsilon = 10^{-5}$		$\epsilon = 10^{-6}$		$\epsilon = 10^{-7}$	
	$L_2$ error	Relative mean error	$L_2$ error	Relative mean error	$L_2$ error	Relative mean error
1	$2.56 \times 10^{-1}$	$3.99 \times 10^{-2}$	$2.56 \times 10^{-1}$	$3.98 \times 10^{-2}$	$2.56 \times 10^{-1}$	$3.98 \times 10^{-2}$
2	$7.53 \times 10^{-2}$	$2.23 \times 10^{-3}$	$7.57 \times 10^{-2}$	$2.55 \times 10^{-3}$	$7.57 \times 10^{-2}$	$2.65 \times 10^{-3}$
3	$1.07 \times 10^{-2}$	$4.02 \times 10^{-4}$	$1.12 \times 10^{-2}$	$2.25 \times 10^{-4}$	$1.13 \times 10^{-2}$	$1.46 \times 10^{-4}$

is the relative integration error. As expected, the refinement of the ASGC does not improve the accuracy of the interpolation error within each expansion order. This is consistent with the previous results that when HDMR is not converged, the overall error is dominated by the truncation error. On the other hand, the integration value converges with a third-order expansion and for this case refining the ASGC improves the accuracy of the mean value. This suggests that the expansion order and the refinement of ASGC should be increased simultaneously to achieve a satisfactory accuracy, which is consistent with the results reported in [37].

Since each dimension may weigh unequally in this function, it is also interesting to compare the performance of HDMR with that of adaptive methods, i.e. adaptive HDMR and ASGC. The adaptive HDMR is combined with ASGC as described in Section 4.3. We fix  $\theta_2 = 10^{-4}$  while varying  $\theta_1$ . In addition, we choose the same  $\varepsilon = 10^{-6}$  for all three methods (conventional fixed-order HDMR, adaptive HDMR and ASGC). The results are given in Table 4. For conventional HDMR, we need about 4 million collocation points to obtain an accurate result. On the other hand, it is seen that we can arrive at the same integration error as that of conventional HDMR and ASGC with much less number of collocation points by using adaptive HDMR. However, the interpolation error of adaptive HDMR is larger than that of the other two methods. This is expected since our error indicator for the important component functions is based on the mean value and thus it generally favors the strong interaction between those dimensions that impact the mean of the output. Therefore, due to the multiplicative nature of the function, we need to include all the component functions to compute an accurate value.

This example shows that HDMR may not be useful for interpolating arbitrary mathematical functions but it may have a good convergence property for the approximation of integrals. Although the lack of the importance of higher-order effects for constructing the approximation of input–output relations for most deterministic physical systems is general [24–28], this feature for the interpolation of stochastic systems deserves further investigation in the next few examples. In addition, the relation between the convergence of the output statistics and the expansion order of HDMR is also important which has not been reported before.

In Fig. 4, we also investigate the effects of different choices of the reference point. It is shown that the results are indeed more accurate for a fixed-order expansion if the reference point is near the center of the domain. Therefore, in the remaining of the examples, we always take the reference point as the mean of the input random vector.

#### 5.4. Example 3

The final example in this set entails calculation of the mean and standard deviation of the output

$$f(\mathbf{X}) = \frac{1}{1 + \sum_{i=1}^{10} \alpha_i X_i}, \tag{47}$$

where the random input  $X_i = \sigma Y_i$  and  $Y_i$  are i.i.d. uniform random variables in  $[-\sqrt{3}, \sqrt{3}]$ ,  $i = 1, \dots, 10$ . Therefore, the parameter  $\sigma$  controls the standard deviation (std) of the input. The coefficients  $\alpha_i$ ,  $i = 1, \dots, 10$  adjust the weight of each dimension. The HDMR expansion is employed to compute the mean and standard deviation of the output.

First, an isotropic case is considered by setting  $\alpha_i = 0.1$ ,  $i = 1, \dots, 10$ , i.e. each dimension weighs equally. The results are plotted in Fig. 5 for increasing values of standard input deviation. The relative errors are defined the same as before where the reference solution is taken from  $10^6$  MC samples. Here, conventional (fixed-order) HDMR is used where the error threshold is  $\varepsilon = 10^{-6}$ . From the figure, it is seen that with increasing  $\sigma$ , a higher-order expansion is needed to obtain an acceptable accuracy of order  $\mathcal{O}(10^{-3})$ . On the other hand, when  $\sigma$  is small, only second-order expansion is enough to give us accurate results. Even first-order expansion is accurate when  $\sigma \leq 0.1$ . When  $\sigma \geq 0.7$ , fourth-order expansion is not enough and thus higher-order terms in the HDMR expansion are needed. The higher the input standard deviation is, the stronger the correlation effects are among the dimensions. Therefore, higher-order expansion is needed to capture these cooperative effects. In function Eq. (46), the input is uniform distribution [0,1]. Its input standard deviation is about 0.289, which is not very large. This explains why its mean converges after a third-order expansion.

The interpolation error is also given in Fig. 6. As expected, due to the non-linear nature of the function, higher-order HDMR expansions usually give better accuracy. But at the same time, the interpolation error for a fixed-order expansion also increases with increasing  $\sigma$ . It is also noted that, as for the integration case, a smaller  $\sigma$  has the effect of reducing the number of the effective dimensions of the function. For example, when  $\sigma = 0.3$ , the relative error is about  $10^{-3}$  when using only a second-order HDMR.

**Table 4**  
Comparison of performance of conventional (fixed-order) HDMR, adaptive HDMR and ASGC.

	# Terms	# Points	$\epsilon_{\text{interpolation}}$	$\epsilon_{\text{integration}}$
5th HDMR	638	4,712,870	$5.65 \times 10^{-4}$	$1.62 \times 10^{-4}$
HDMR: $\theta_1 = 10^{-3}$	78	83,400	$6.23 \times 10^{-2}$	$8.72 \times 10^{-4}$
HDMR: $\theta_1 = 10^{-4}$	140	220,930	$1.47 \times 10^{-2}$	$1.28 \times 10^{-4}$
ASGC: $\varepsilon = 10^{-6}$	N/A	305,670	$4.23 \times 10^{-4}$	$1.28 \times 10^{-4}$

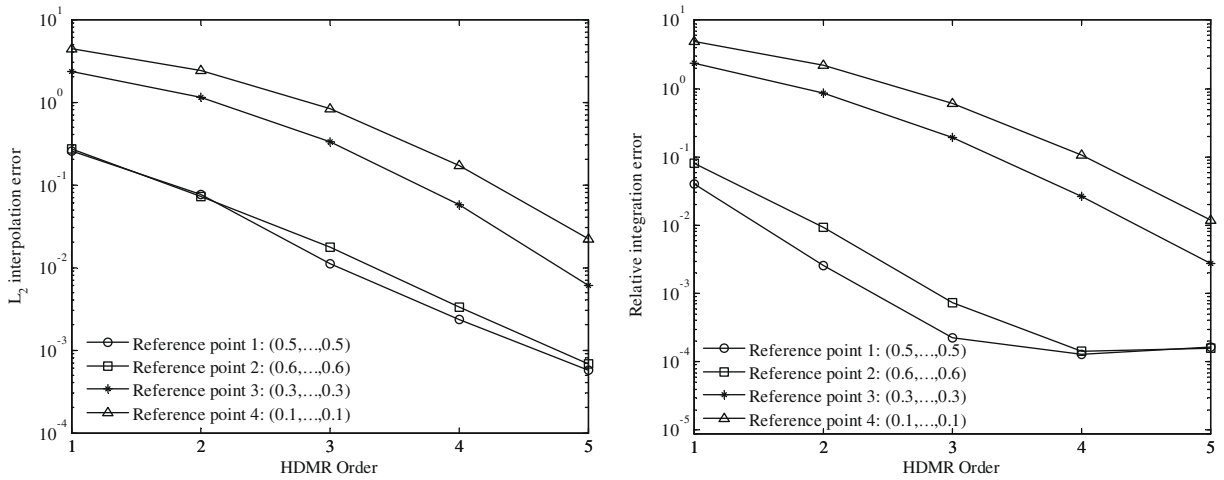


Fig. 4. Error convergence for four different reference points.

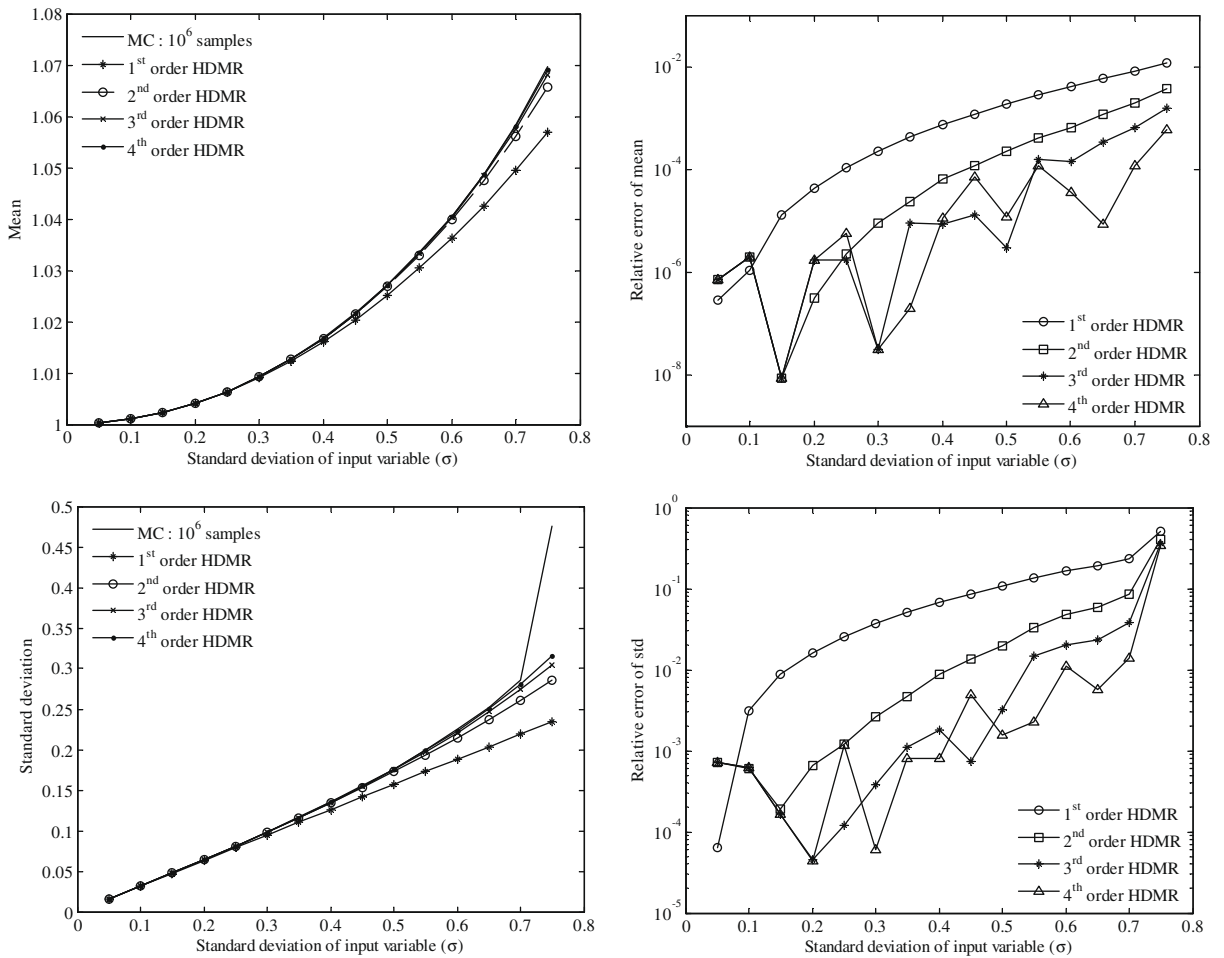


Fig. 5. Mean and standard deviation of the function in Eq. (47) for increasing values of input standard deviation using conventional (fixed-order) HDMR. Top left: mean; Top right: error of mean; Bottom left: standard deviation; Bottom right: error of standard deviation.

Next, we consider two anisotropic cases. For Case 1,  $\alpha_i = \frac{0.1}{2^{i-1}}, i = 1, \dots, 10$ . The ratio between the smallest coefficient and the largest one is about 0.002. For Case 2,  $\alpha_i = \frac{0.1}{10^{i-1}}, i = 1, \dots, 10$ . The ratio between the smallest coefficient and the largest

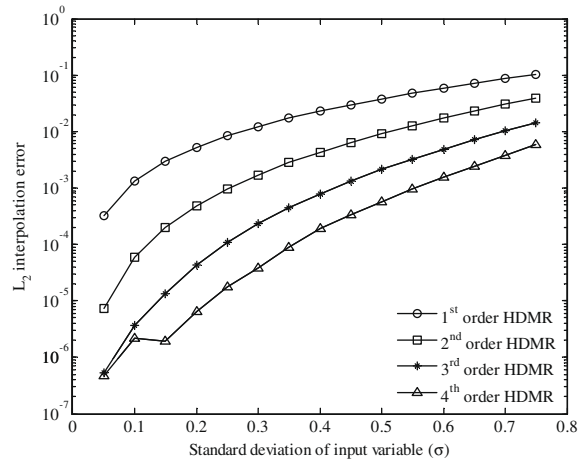


Fig. 6. Interpolation error of the function in Eq. (47) using conventional (fixed-order) HDMR with different expansion orders.

one is about  $10^{-9}$ . Thus, Case 1 refers to an anisotropic problem with small differences between dimensions while Case 2 refers to a highly anisotropic problem where the first four dimensions are the most important. In these two cases, we again fix the ASGC threshold  $\varepsilon = 10^{-6}$  and choose a rather large input standard deviation  $\sigma = 2.0$ . The reference solution is still taken from  $10^6$  Monte Carlo samples. The results for Cases 1 and 2 are plotted in Figs. 7 and 8, respectively. In the left plot of Fig. 7, it is seen that the mean and standard deviation converge even for such a large  $\sigma$ . The interpolation error achieves an order of  $10^{-4}$  with only a fourth-order HDMR. Therefore, the different weights between dimensions result in reduction of the number of effective dimensions in the HDMR expansion. This is more obvious in the left plot of Fig. 8 where the mean and std errors converge after a second-order expansion and the interpolation error converges after a third-order expansion. This can be explained as follows. If the weights of some dimensions are much larger than those of others, then these dimensions have most of the impact on the output. In this case, only those component functions which consist of these dimensions provide most of the contribution to HDMR. If the number of important dimensions is small, then less component functions are needed and this leads to an accurate low-order HDMR expansion.

Since each dimension is given a different weight, we also use adaptive HDMR. In the plots on the right of Figs. 7 and 8, we compare the HDMR (conventional and adaptive) convergence rates for Cases 1 and 2, respectively, with those of ASGC. To plot the convergence of conventional (fixed-order) HDMR, we increase the expansion order from 1 to 5 (each symbol in the figures denotes an expansion order). The convergence of adaptive HDMR is plot by decreasing  $\theta_1$  (each symbol in the figures corresponds to a different  $\theta_1$  value). To plot the convergence of ASGC, we plot the error at each interpolation level when constructing the grid level by level. It is seen that for Case 2 adaptive HDMR is much better than both conventional HDMR and ASGC. On the other hand, in Case 1, ASGC is better than the HDMR methods in terms of interpolation. This is ex-

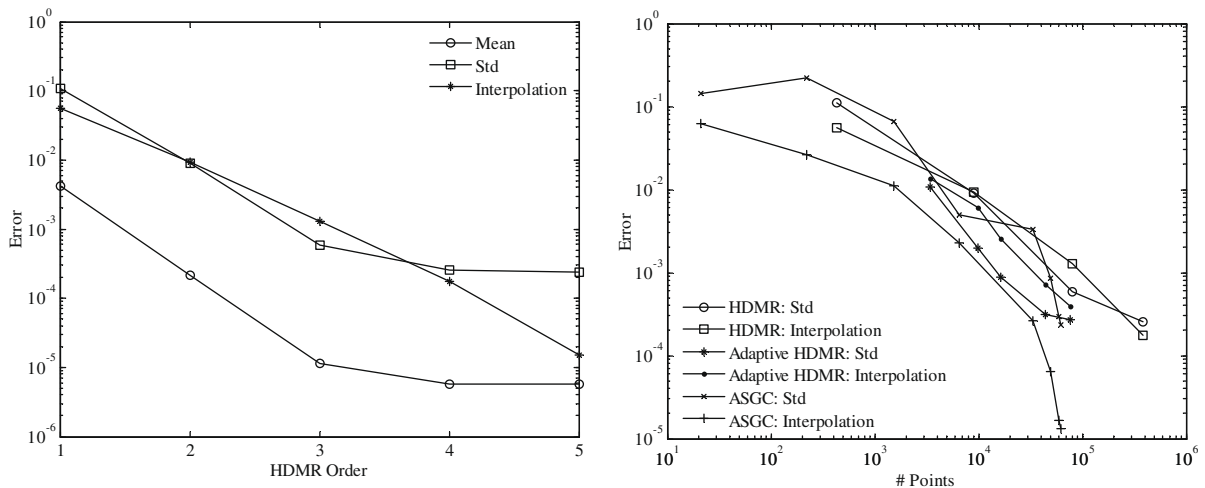
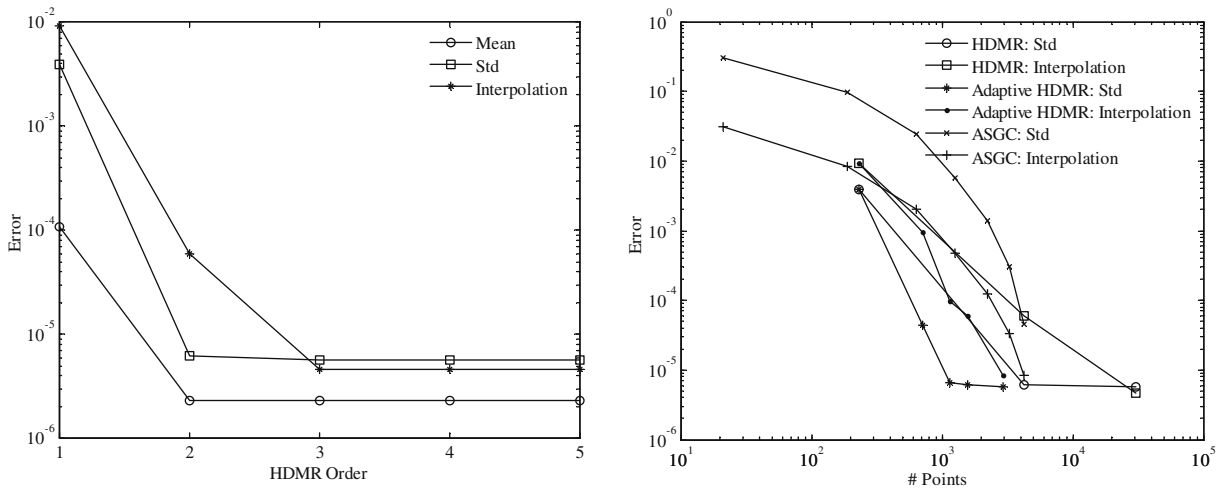


Fig. 7. Error convergence of the anisotropic Case 1 when  $\alpha_i = 0.1/2^{i-1}, i = 1, \dots, 10$  with  $\sigma = 2.0$ . Left: conventional (fixed-order) HDMR. Right: comparison between conventional (fixed-order) HDMR, adaptive HDMR and ASGC.



**Fig. 8.** Error convergence of anisotropic Case 2 when  $\alpha_i = 0.1/10^{i-1}, i = 1, \dots, 10$  with  $\sigma = 2.0$ . Left: conventional (fixed-order) HDMR. Right: comparison between conventional (fixed-order) HDMR, adaptive HDMR and ASGC.

pected since, in such a high  $\sigma$  case, there is no significant difference between dimensions and we need a higher-order expansion to capture the interaction effects.

Tables 5 and 6 show the total number of collocation points and also the number of expansion terms used in HDMR for different  $\theta_1$ . It is noted that adaptive HDMR requires much less expansion terms and thus less collocation points than conventional HDMR, especially in Case 2. It is also interesting to note that to achieve the same accuracy, the number of expansion terms in Case 2 is less than that of case 1. This is due to the strong anisotropic weights such that only the first five dimensions are important. Therefore, only those terms which involve these dimensions are constructed by adaptive HDMR. In Fig. 9, for both cases we also plot the weights, which are defined in Eq. (40) for each first-order component function indicating the importance of each dimension. It can be seen that the weights decrease quickly with the indices of the dimensions. In Case 1, the number of important dimensions are 7, 9 and 10 for  $\theta_1 = 10^{-5}, 10^{-6}$  and  $10^{-7}$ , respectively. In Case 2, the number of important dimensions are 3, 4 and 5 for  $\theta_1 = 10^{-6}, 10^{-7}$  and  $10^{-9}$ , respectively.

Overall, the HDMR reveals the correlations among the input variables as reflected upon the output. Each order- $l$  terms introduce the correlated effects of  $l$ -input variables into the expansion. Therefore, the order of HDMR expansion or the total number of component functions depends on the cooperative effects among the input dimensions, which further depends on the input variability and the importance of each dimension as demonstrated through this example set. In general, higher-order expansion will give better accuracy since it captures more correlation effects. However, as shown in this example, HDMR is useful if it can represent the output to a good accuracy with a sufficiently low-order expansion. For the case of small input variability and strong anisotropic situation, a low-order expansion can lead to a good accuracy. At the same time, by using adaptive HDMR, we can also significantly reduce the computational cost without sacrificing the accuracy. In the next

**Table 5**  
Comparison of performance of fourth-order HDMR and adaptive HDMR for the anisotropic Case 1 where  $\alpha_i = 0.1/2^{i-1}, i = 1, \dots, 10$ .

	4th HDMR	Adaptive HDMR		
		$\theta_1 = 10^{-5}$	$\theta_1 = 10^{-6}$	$\theta_1 = 10^{-7}$
# Terms	386	37	64	88
# Points	388,891	16,584	44,095	75,877

**Table 6**  
Comparison of performance of third-order HDMR and adaptive HDMR for the anisotropic Case 2 where  $\alpha_i = 0.1/10^{i-1}, i = 1, \dots, 10$ .

	3 <sup>rd</sup> HDMR	Adaptive HDMR		
		$\theta_1 = 10^{-6}$	$\theta_1 = 10^{-7}$	$\theta_1 = 10^{-9}$
# Terms	176	14	17	22
# Points	30,296	1144	1575	2912

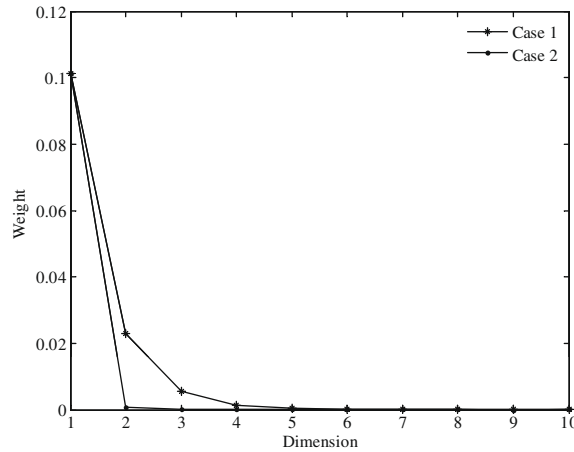


Fig. 9. The decay of the weights of the first-order expansion terms for the two anisotropic cases.

two sections, we will investigate the convergence properties of adaptive HDMR on realistic physical systems and investigate if similar conclusions are obtained.

5.5. Example set II – fluid-mechanics problems

In the following two examples, random fields which are discretized by K-L expansion are introduced to increase the dimension of the stochastic problem. The reference solutions are taken from Monte Carlo simulations. The obtained mean values in these examples compared extremely well with the corresponding MC results for all cases considered and therefore we will focus our discussion only on the standard deviation. The spatial  $L_2$  normalized error of std  $\sigma$  is defined as

$$\epsilon_{L_2} = \frac{\sqrt{\sum_{i=1}^n (\sigma_{\text{HDMR}}(\mathbf{x}_i) - \sigma_{\text{MC}}(\mathbf{x}_i))^2}}{\sqrt{\sum_{i=1}^n \sigma_{\text{MC}}(\mathbf{x}_i)^2}} \tag{48}$$

where  $n$  is the number of grid points in the spatial domain.

5.6. Example 4: flow through random heterogeneous media

In this section, we consider flow through random porous media where the permeability is a random field obtained from the K-L expansion of an exponential covariance function. Through this classical problem, we want to investigate the effects of input variability on the accuracy and convergence of HDMR. The problem is defined as follows:

$$\nabla \cdot \mathbf{u}(\mathbf{x}, \mathbf{Y}) = f(\mathbf{x}), \tag{49}$$

$$\mathbf{u}(\mathbf{x}, \mathbf{Y}) = -K(\mathbf{x}, \mathbf{Y}) \nabla p(\mathbf{x}, \mathbf{Y}), \tag{50}$$

where the source/sink term  $f(\mathbf{x})$  is taken to be deterministic and  $K(\mathbf{x}, \mathbf{Y})$  is the random permeability. The domain of interest is a quarter-five spot problem in a unit square  $D = [0, 1]^2$ . Flow is driven by an injection well at the bottom left corner of the domain and a production well at the top right corner. A mixed finite element method is utilized to solve the forward problem [21].

The log-permeability is taken as zero mean random field with a separable exponential covariance function

$$\text{Cov}(\mathbf{x}, \mathbf{y}) = \sigma^2 \exp\left(-\frac{|\mathbf{x}_1 - \mathbf{y}_1|}{L} - \frac{|\mathbf{x}_2 - \mathbf{y}_2|}{L}\right), \tag{51}$$

where  $L$  is the correlation length and  $\sigma$  is the standard deviation of the random field. The K-L expansion is used to parameterize the field as

$$\mathbf{Y}(\omega) = \log(K(\omega)) = \sum_{i=1}^N \sqrt{\lambda_i} \phi_i(\mathbf{x}) Y_i, \tag{52}$$

where the eigenvalues  $\lambda_i, i = 1, 2, \dots$ , and their corresponding eigenfunctions  $\phi_i, i = 1, 2, \dots$ , can be determined analytically as discussed in [1,5]. The  $Y_i$  are assumed as i.i.d. uniform random variables on  $[-1, 1]$ .

In order to investigate the accuracy and applicability of the proposed HDMR approach, we design a series of numerical runs with different correlation lengths  $L$  and various degrees of spatial variability  $\sigma^2$ . The first three cases aim to investigate

the effects of correlation length ( $L = 1.0, 0.5$  and  $0.25$ ) on the proposed approach. In these cases, the degree of spatial variability is kept at  $\sigma^2 = 1.0$ , which corresponds to a moderately high variability. The next three cases are compared against case 3 when  $L = 0.25$  to examine the impact of the log-permeability variability ( $\sigma^2 = 0.01, 0.25$  and  $2.0$ ) ranging from very low to extremely high variability. Monte Carlo simulations are conducted for the purpose of comparison. For each case, the reference solution is taken from  $10^6$  MC samples and all errors are defined as normalized  $L_2$  errors. In all cases, the threshold  $\theta_2$  for the relative error is fixed at  $\theta_2 = 10^{-4}$ .

Let us first determine the stochastic dimension of our example cases. The eigenvalues and the sum of the eigenvalues as a function of the number of terms included are illustrated in Fig. 10 with three different correlation lengths for the case  $\sigma^2 = 1.0$ . The corresponding eigenfunctions are shown in Fig. 11. Based on these figures, the K-L expansions are truncated after 33, 108 and 500 terms, respectively for  $L = 1.0, 0.5, 0.25$ , which represents  $\approx 95\%$  of the total variance of the exponential covariance function. The truncation level for the expansion does not change for a fixed correlation length. Therefore, in all cases, the number of stochastic dimensions is  $N = 33, 108$  and  $500$ , respectively for  $L = 1.0, 0.5$  and  $0.25$ . In these cases, the ratio between the smallest eigenvalue and the largest eigenvalue is about  $10^{-3}$  which is similar to the moderate anisotropic Case 1 in Section 5.4. According to previous results on mathematical functions, we would expect that the convergence of the HDMR expansion depends on the input variability and that HDMR can deal with a moderately high stochastic input standard deviation.

### 5.6.1. Effect of correlation length

We fix  $\sigma^2 = 1.0$  and consider three different correlation lengths at  $L = 1.0, 0.5$  and  $0.25$ . In this way, the input variability is fixed and the change of correlation length adjusts the weights of each random dimension. Thus, we want to investigate the effect of the smoothness of the stochastic space on the accuracy of the HDMR expansion as we did in Section 5.4.

We decrease  $\varepsilon$  and  $\theta_1$  simultaneously until the  $L_2$  normalized errors reach an order of  $\mathcal{O}(10^{-3})$ . It is interesting to note that these computed errors are achieved with the same  $\varepsilon = 10^{-6}$  and  $\theta_1 = 10^{-4}$  for all three correlation lengths. In Fig. 12, we compare the standard deviation of the  $v$  velocity-component along the line  $y = 0.5$  with the results from the MC simulation. It is seen that the two results compare extremely well, where the errors are  $1.46 \times 10^{-3}$ ,  $1.19 \times 10^{-3}$  and  $1.39 \times 10^{-3}$ , respectively for  $L = 1.0, L = 0.5$  and  $L = 0.25$ .

To investigate the convergence of HDMR, we fix  $\varepsilon = 10^{-6}$  while varying  $\theta_1$ . The PDFs of the  $v$  velocity-component at point  $(0,0.5)$ , where the standard deviation is large as in Fig. 12, are shown in Fig. 13. Each PDF is generated by plotting the kernel density estimate of 10000 output samples through sampling the input space and computing the output value through the HDMR approximation. When  $\theta_1 = 10^{-2}$ , the weights of all first-order terms are smaller than the threshold and thus there are no higher-order terms. It is seen that the results from only the first-order expansion are not accurate in all three cases which is consistent with the result in Fig. 7. This may be explained intuitively as follows. The spatial variability  $\sigma^2$  determines the total input variability, which further determines the correlation effects among the input variables. The larger the input variability is, the stronger the correlation effects are. The role of HDMR component functions is to capture these input effects upon the output. In other words, the number of component functions needed depends on the input variability. The higher the input variability is, the more component functions are needed for a fixed stochastic dimension. For low-input variability, even first-order expansion may be accurate enough no matter what the stochastic dimension is. In our case,  $\sigma^2 = 1.0$  represents a rather high-input variability. Higher-order terms are therefore needed to capture these effects whereas only first-order terms are not enough. The number of important dimensions is shown in Table 7. By decreasing  $\theta_1$ , more dimensions whose weights defined in Eq. (40) are larger than  $\theta_1$  become important and thus more second-order terms ap-

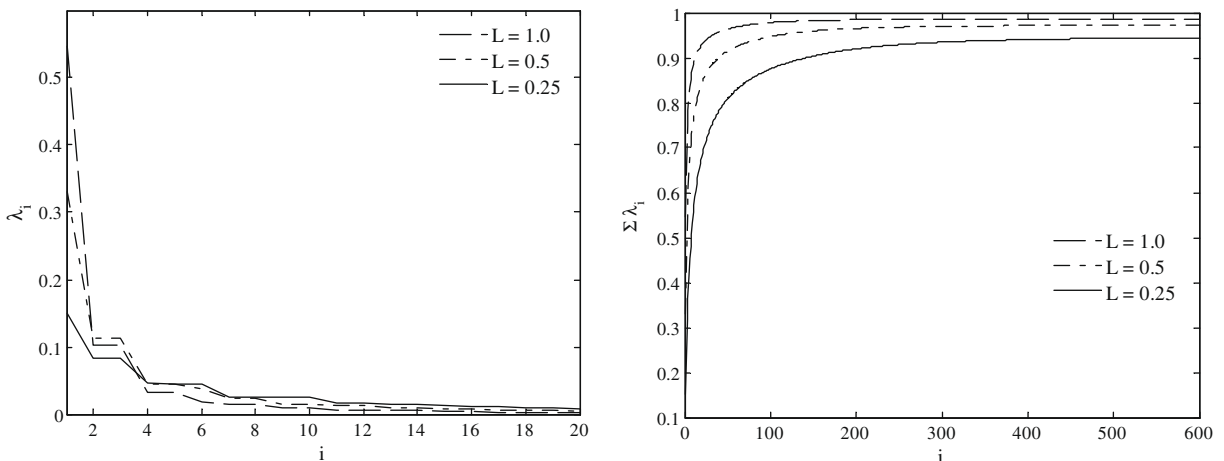


Fig. 10. Series of eigenvalues and their finite sums for three different correlation lengths at  $\sigma^2 = 1.0$ .

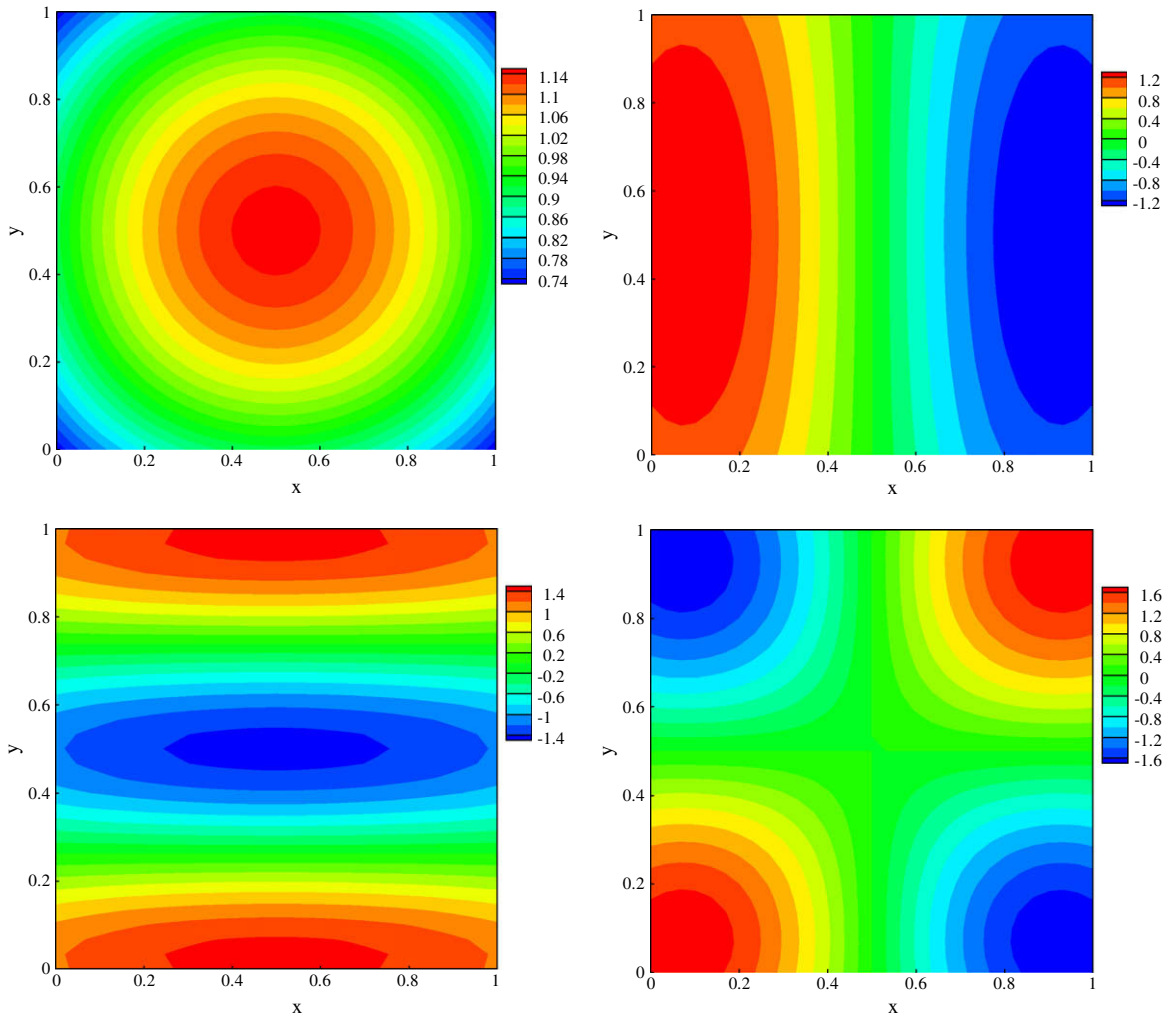


Fig. 11. Four different eigenfunctions for  $L = 1.0$  and  $\sigma^2 = 1.0$ . Top left:  $\phi_1$ ; Top right:  $\phi_2$ ; Bottom left:  $\phi_5$ ; Bottom right:  $\phi_6$ .

pear. This means more correlation effects are included in the expansion and thus better accuracy. The number of component functions is 287, 889 and 2271 while for the full second-order expansion it is 562, 5887 and 125,251, respectively. Thus, the advantage of using adaptive HDMR is obvious, especially for  $N = 500$ . As expected, all the results converge to those obtained from the MC simulation with decreasing  $\theta_1$ . The computed PDFs indicate that the corresponding HDMR approximations are indeed very accurate. Therefore, we can obtain any statistic from this stochastic reduced-order model, which is an advantage of the current method over the MC method.

The convergence of the  $L_2$  normalized error with respect to the total number of collocation points is shown in Fig. 14 by fixing  $\theta_1 = 10^{-4}$ . The error plots are obtained by decreasing the threshold  $\varepsilon$  used in the ASGC. Although different correlation lengths result in different truncated stochastic dimensions from the K-L expansion, it is interesting to note that we still have algebraic convergence rates and they are nearly the same for all three cases. This may be explained using Theorem 1. The input variability is the same and so is the superposition dimension. Thus, the constant in Eq. (36), which only depends on the effective dimensions, is nearly the same. In addition, the error in Eq. (36) exhibits a linear dependence on the threshold  $\varepsilon$  and as we know the convergence rate of the sparse grid collocation method is algebraic [17,23]. Thus, the convergence plot here indeed exhibits algebraic rate as indicated from Theorem 1.

In order to further verify the results discussed in this section, we investigate the effect of the spatial variability in the next section.

### 5.6.2. Effect of the spatial variability $\sigma^2$

In this section, we fix the correlation length at  $L = 0.25$  such that the weight of each dimension from the K-L expansion is nearly the same. Then we explore the effects of the spatial variability  $\sigma^2$ , from very small variability  $\sigma^2 = 0.01$  to very high

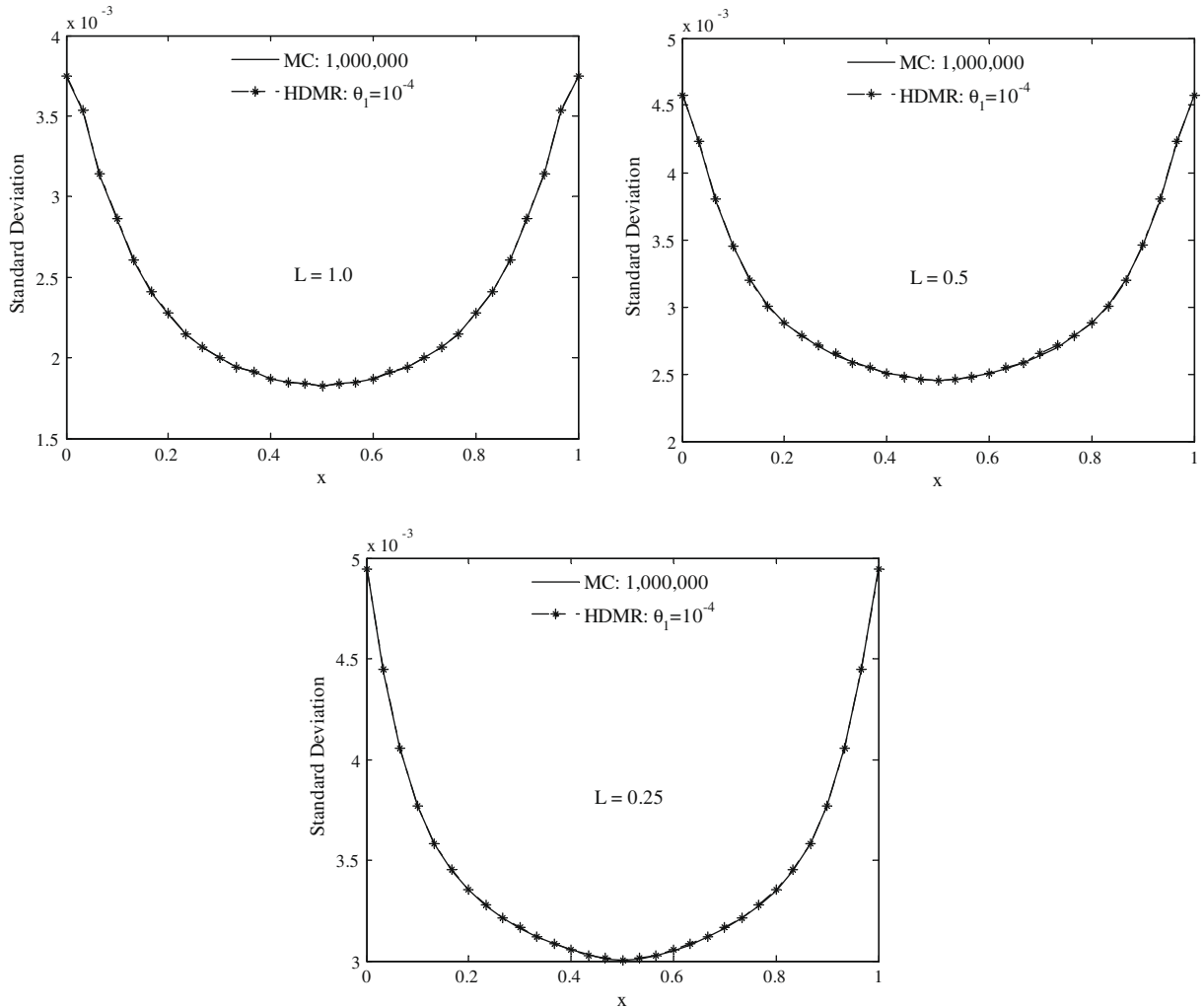


**Fig. 12.** Standard deviation of the  $v$  velocity-component along the cross section  $y = 0.5$  for different correlation lengths where  $\sigma^2 = 1.0$ ,  $\varepsilon = 10^{-6}$  and  $\theta_1 = 10^{-4}$ .

variability  $\sigma^2 = 2.0$ . The number of stochastic dimensions is  $N = 500$ . For such a nearly isotropic situation, as indicated in Fig. 5, it is expected that the accuracy of HDMR depends on the input spatial variability.

Fig. 15 compares the standard deviation of the  $v$  velocity-component along the line  $y = 0.5$  with the results obtained from the MC simulation. Again, we obtain very good comparison where the errors are  $8.08 \times 10^{-4}$ ,  $7.37 \times 10^{-4}$  and  $2.86 \times 10^{-3}$  for  $\sigma^2 = 0.01$ ,  $\sigma^2 = 0.25$  and  $\sigma^2 = 2.0$ , respectively. Comparing with the result when  $\sigma^2 = 1.0$ , it can be seen that the error in standard deviation increases with increasing input variability which again verifies our previous results in Fig. 5. However, we can still obtain an acceptable accuracy even when the spatial variability is as high as  $\sigma^2 = 2.0$ . It is interesting to note that the threshold  $\varepsilon$  needed to achieve the desired accuracy is smaller for  $\sigma^2 = 0.01$  and  $0.25$  than for  $\sigma^2 = 1.0$ . This is due to the small correlation length and low input variability which results in a rather smooth stochastic space such that the hierarchical surpluses decrease very fast. Therefore, we need a much smaller  $\varepsilon$  to trigger the adaptivity otherwise the refinement of ASGC for each sub-problem stops earlier. This also shows the ability of ASGC to detect the smoothness of the stochastic space. The increase of the spatial variability also results in the increase of the magnitude of the standard deviation from  $\sigma^2 = 0.01$  to  $\sigma^2 = 2.0$  in Fig. 15, i.e. increasing of the variability in the solution.

Similarly, the convergence of the corresponding PDFs is given in Fig. 16. For the case  $\sigma^2 = 0.01$ , we show the convergence with respect to  $\varepsilon$  instead. This is because the first-order expansion is accurate enough to represent the solution due to the rather low input variability as expected. Even when the value of  $\theta_1$  is as small as  $10^{-4}$ , the weights of all the first-order terms from Eq. (40) are still smaller than the threshold. Therefore, there is no need to include second-order terms. Due to the small variability, even a smaller  $\varepsilon$  can give us a very accurate result as shown in the figure. Compared with Fig. 13, although second-order terms are still needed for the cases  $\sigma^2 = 0.25$  and  $2.0$ , the PDFs from the first-order terms are not apart from the

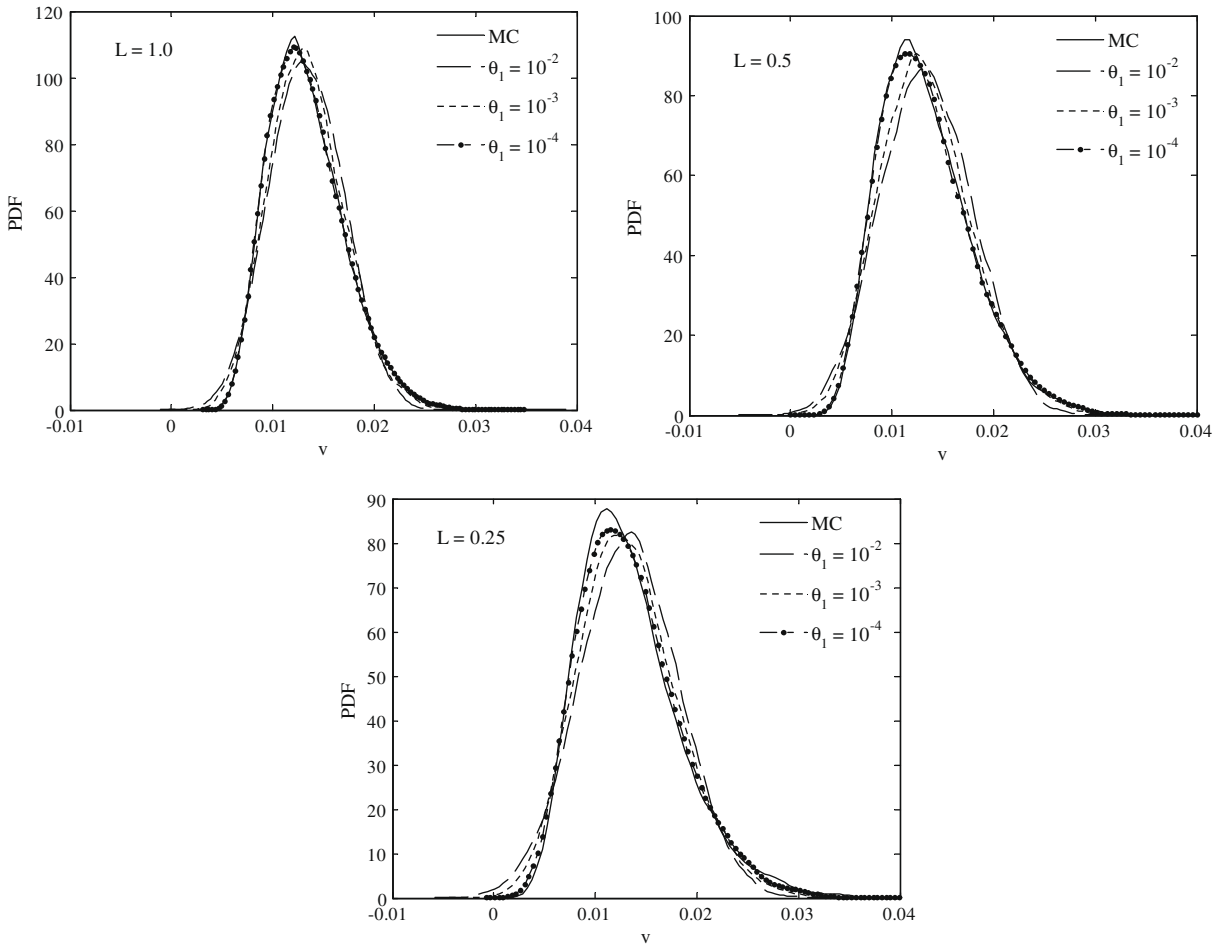


Fig. 13. PDF of  $v$  velocity-component at point (0.05) for different correlation lengths, where  $\sigma^2 = 1.0$  and  $\varepsilon = 10^{-6}$ .

Table 7

Number of important dimensions  $N_i$  and component functions  $N_c$  for different  $\theta_1$ .

$\theta_1$	$L = 1.0$		$L = 0.5$		$L = 0.25$	
	$N_i$	$N_c$	$N_i$	$N_c$	$N_i$	$N_c$
$10^{-2}$	0	34	0	109	0	501
$10^{-3}$	5	44	8	137	11	556
$10^{-4}$	23	287	40	889	60	2271

MC results for the cases  $\sigma^2 = 0.25$  and  $\theta_1 = 10^{-2}$  when the input variability is moderately high. On the other hand, for  $\sigma^2 = 2.0$ , the result from the first-order HDMR expansion ( $\theta_1 = 10^{-2}$ ) deviates significantly from that of the MC results. Indeed, comparing all four cases when  $L = 0.25$ , it is clear that the PDFs from the first-order expansion deviate gradually from the MC results with increasing input variability  $\sigma^2$ . This reflects that the correlation effects become significant and therefore more higher-order terms are needed to capture these effects, which is again consistent with the result in Fig. 6. The improvement of the results is obvious as more terms are included with decreasing  $\theta_1$ . This numerically verifies our previous discussion that the number of component functions needed depends on the input variability. There are 501, 879 and 2271 component functions for  $\sigma^2 = 0.01, 0.25$  and  $2.0$ , respectively. Correspondingly, the total number of collocation points are 9337, 74,127, and 249,329.

The convergence of the  $L_2$  normalized error with respect to the total number of collocation points is shown in Fig. 14 by decreasing  $\varepsilon$  in the ASGC. As expected, the convergence rates deteriorate with increasing  $\sigma^2$ . For  $\sigma^2 = 0.01$ , the convergence rate is nearly of the order of  $\mathcal{O}(M^{-2.87})$ . This is because first-order HDMR expansion is used and the number of collocation points used in the first-order terms is much lower than that in higher-order terms. The convergence rate for the case

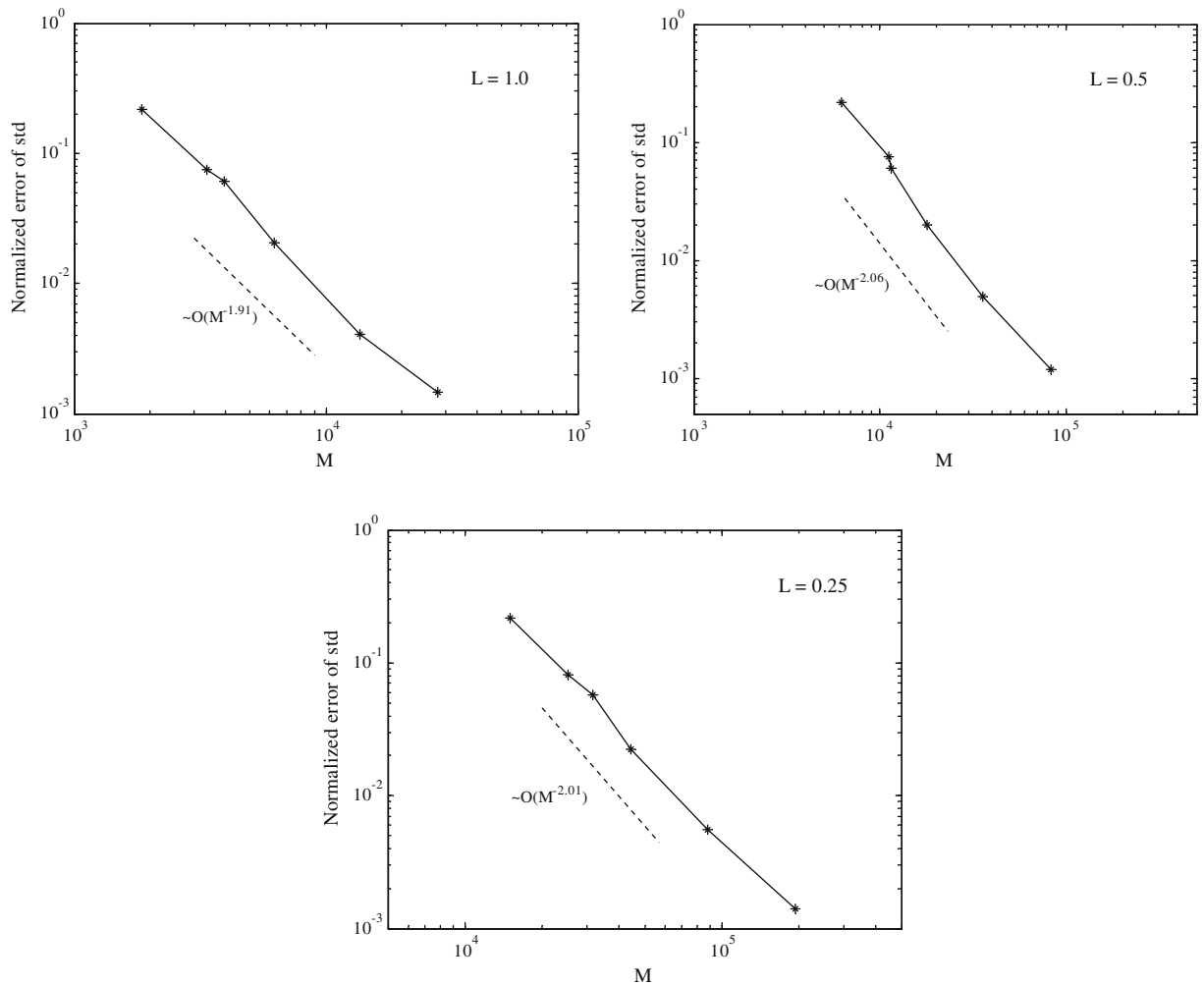


**Fig. 14.** Convergence of the  $L_2$  normalized errors of the standard deviation of the  $v$  velocity-component for different correlation lengths, where  $\sigma^2 = 1.0$  and  $\theta_1 = 10^{-4}$ .

$\sigma^2 = 2.0$  is the lowest among all the cases examined so far. However, it is still better than the theoretic MC rate  $\mathcal{O}(M^{-0.5})$  and the results compare well with that of MC. Comparing all four cases when  $L = 0.25$ , it is seen that although the stochastic space is smooth, the convergence rate still decreases with increasing spatial variability. Thus, as discussed before, the number of component functions needed for a fixed stochastic dimension depends more on the input variability for such situation. This provides us a very useful guideline to set up the parameters when applying HDMR to realistic stochastic problems. On the other hand, the regularity of the stochastic space can be effectively resolved with the ASGC method. The proposed method is indeed a very powerful and versatile method to address stochastic PDE problems.

### 5.6.3. Effect of choices of the reference points $\bar{\mathbf{Y}}$

Here, we also investigate the effect of the reference points  $\bar{\mathbf{Y}}$  on the convergence of the adaptive HDMR expansion when  $\sigma^2 = 1.0$  and  $L = 1.0$  as discussed in Section 4.2.1. We fix  $\varepsilon = 10^{-6}$  and vary  $\theta_1$ . The error convergence for three different reference points is shown in Fig. 18. As expected, when the reference point is far from the mean point, the convergence rate is quite slow and many more points are required to achieve a good accuracy.

In Table 8, we also tabulate the relevant parameters. It is seen from the table and Fig. 18 that when the reference point  $\bar{\mathbf{Y}} = (0.5, \dots, 0.5)$ , it requires the least number of component functions and thus collocation points to achieve an error of order  $\mathcal{O}(10^{-3})$ . When the reference point is far from the center, higher-order expansion is needed to obtain an accurate result. However, when  $\bar{\mathbf{Y}} = (0.1, \dots, 0.1)$ , the error is  $3.82 \times 10^{-2}$  even when using a fourth-order expansion. Thus, we need to increase the expansion order or decrease  $\theta_1$ . This will significantly increase the computational cost. Overall, the result of HDMR is sensitive to the choice of reference point. According to our experience, the mean vector can always give us a satisfied result with much less computational cost. It is also interesting to note that when  $\bar{\mathbf{Y}} = (0.6, \dots, 0.6)$ , in order to achieve an error of

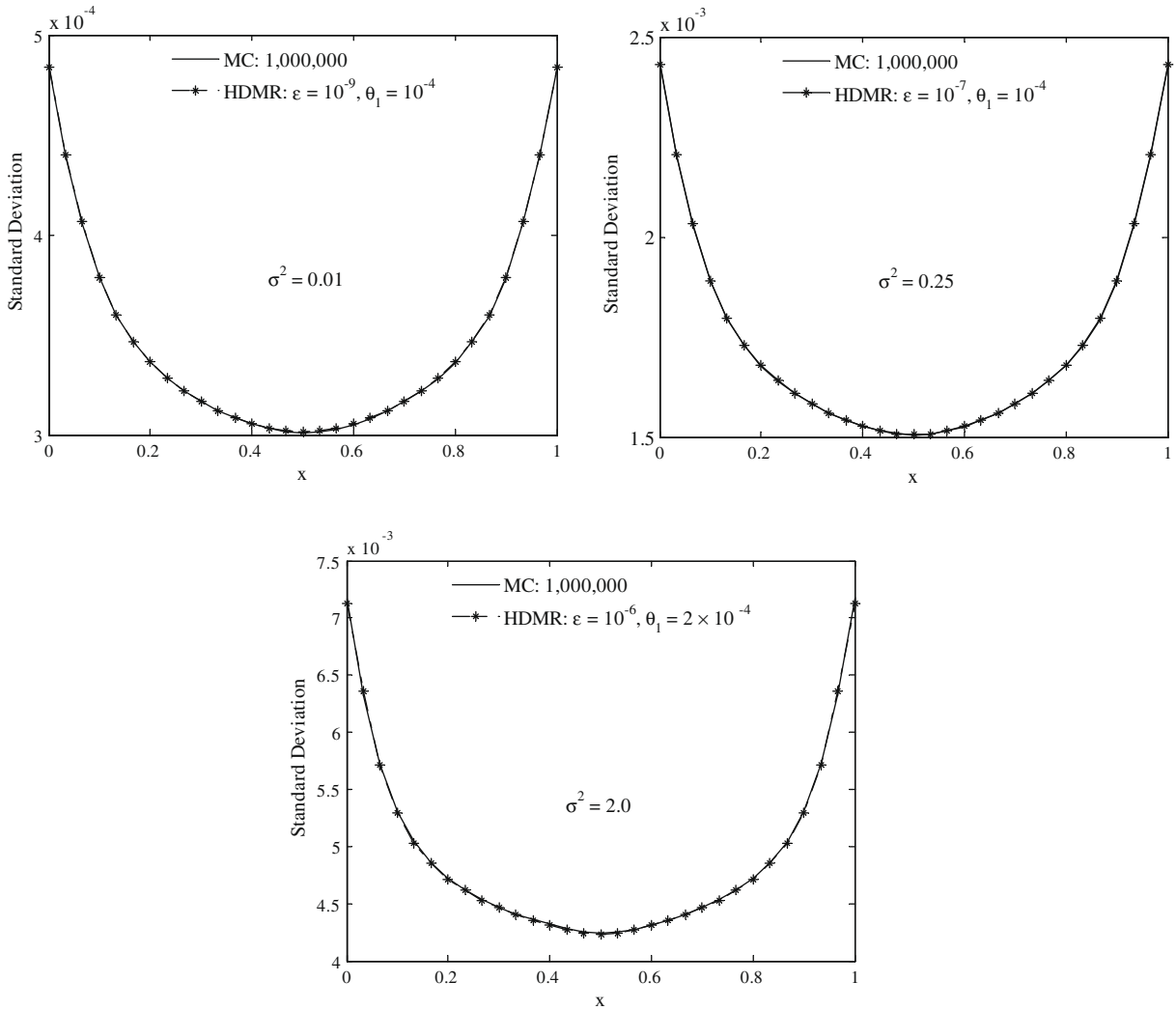


Fig. 15. Standard deviation of the  $v$  velocity-component along the cross section  $y = 0.5$  for different  $\sigma^2$ , where  $L = 0.25$  and  $N = 500$ .

order  $\mathcal{O}(10^{-3})$ , the number of component functions is 880 while the number is 6018 when using conventional HDMR. This again shows the advantage of the adaptive HDMR method.

Finally, it is emphasized here that using the ASGC or CSGC methods alone as in [23] to solve these high-dimensional problems is not feasible due to the following two reasons. At first, the number of needed collocation points is significant for such high-dimensional cases and the convergence rate is very small due to the logarithmic term shown in the error estimation. For example, for  $N = 500$ , the number of points is 167,169,001 for a third-level interpolation. Secondly, there is a need for large memory storage to store all the high-dimensional multi-indices. Therefore, we are not able to compare the results shown in this paper with results that can be obtained directly from the ASGC. However, through the numerical examples, it is shown that the method presented here is indeed a useful tool for solving high-dimensional stochastic problems.

### 5.7. Example 5: stochastic natural convection problem with random boundary conditions

It is interesting to also solve non-linear transient SPDEs using HDMR to investigate if the effective dimensions depend on the type of SPDE. In the following example, a stochastic natural convection problem in a closed cavity is considered. The problem is to find stochastic functions that describe the velocity  $\mathbf{u} \equiv \mathbf{u}(\mathbf{x}, t, \omega) : D \times [0, T] \times \Gamma \rightarrow \mathbb{R}^2$ , pressure  $p \equiv p(\mathbf{x}, t, \omega) : D \times [0, T] \times \Gamma \rightarrow \mathbb{R}$  and temperature  $\theta \equiv \theta(\mathbf{x}, t, \omega) : D \times [0, T] \times \Gamma \rightarrow \mathbb{R}$ , such that the following equations are satisfied:

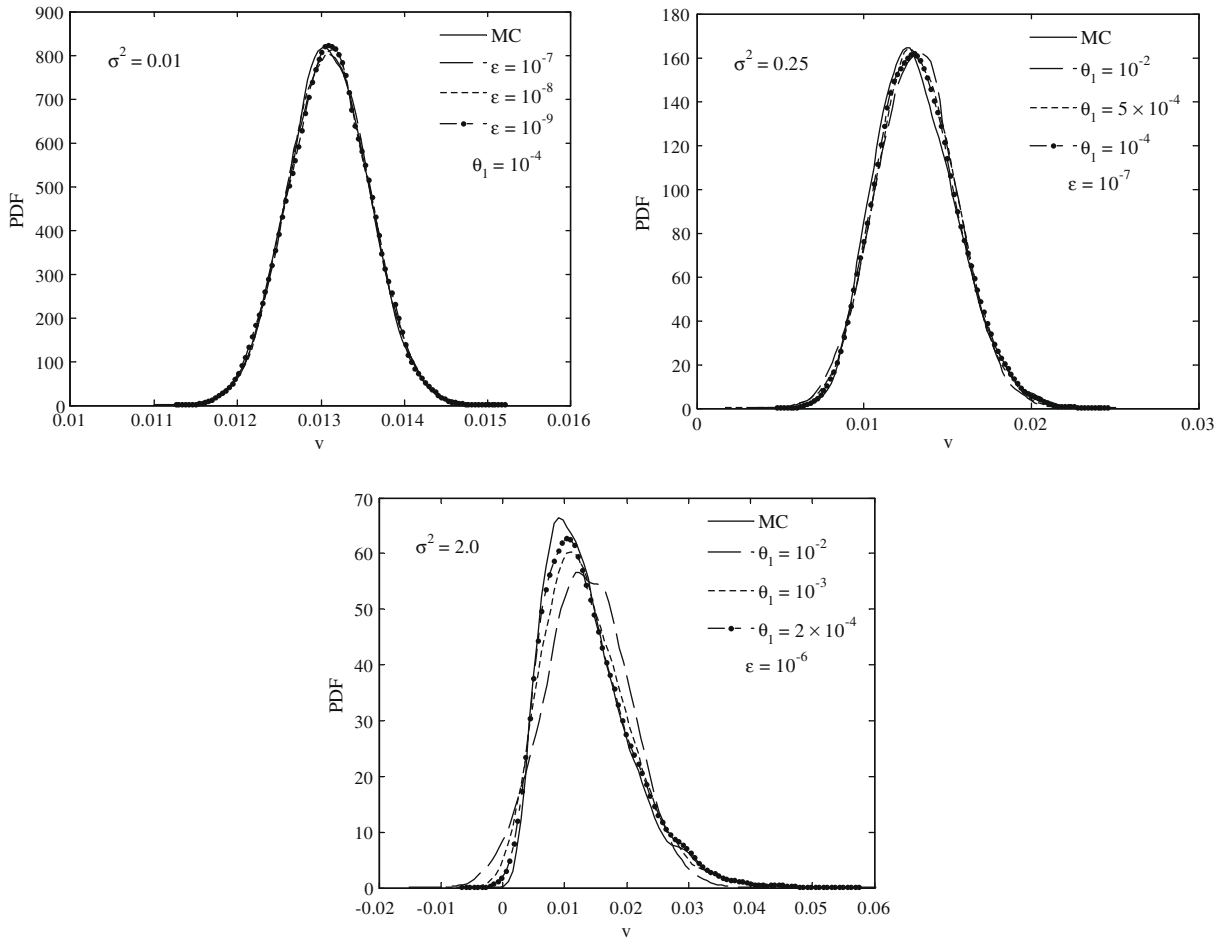


Fig. 16. PDF of the  $v$  velocity-component at point  $(0,0.5)$  for different  $\sigma^2$ , where  $L = 0.25$  and  $N = 500$ .

$$\nabla \cdot \mathbf{u}(\cdot, \omega) = 0, \quad \text{in } D \times [0, T] \times \Gamma, \tag{53}$$

$$\frac{\partial \mathbf{u}(\cdot, \omega)}{\partial t} + \mathbf{u}(\cdot, \omega) \cdot \nabla \mathbf{u}(\cdot, \omega) = -\nabla p(\cdot, \omega) + Pr \nabla^2 \mathbf{u}(\cdot, \omega) + F(\mathbf{u}(\cdot, \omega), \theta(\cdot, \omega)), \quad \text{in } D \times [0, T] \times \Gamma, \tag{54}$$

$$\frac{\partial \theta(\cdot, \omega)}{\partial t} + \mathbf{u}(\cdot, \omega) \cdot \nabla \theta(\cdot, \omega) = \nabla^2 \theta(\cdot, \omega), \quad \text{in } D \times [0, T] \times \Gamma. \tag{55}$$

where  $F(\mathbf{u}(\cdot, \omega), \theta(\cdot, \omega))$  is the forcing function in the Navier–Stokes equations and  $Pr$  is the Prandtl number of the fluid. In the problems considered later,  $F(\mathbf{u}, \theta)$  is the Boussinesq approximated buoyant force term  $-RaPr\theta\mathbf{g}$ , where  $Ra$  is the thermal Rayleigh number and  $\mathbf{g}$  is the gravity vector.

For ease of analysis, we consider a non-dimensional form of the governing equations. The physical domain is taken to be a closed cavity  $[0, 1]^2$ . The Prandtl number  $Pr$  is set to 1.0 and the thermal Rayleigh number  $Ra$  is set to 1000. The deterministic governing equations are solved using the second-order stabilized projection finite element method developed in [12]. The spatial domain is discretized using  $30 \times 30$  bilinear quadrilateral finite elements. Each deterministic simulation is performed until steady-state is reached. No slip boundary conditions are enforced on all four walls. The left wall is maintained at a higher mean temperature of 0.5. The temperature at different points on the left wall is correlated. This is physically feasible through, say, a resistance heater, where the mean temperature remains constant, but material variations cause local fluctuations from this mean temperature. We assume this correlation is a Gaussian correlation function:

$$\text{Cov}(y_1, y_2) = \sigma^2 \exp\left(-\frac{|y_1 - y_2|^2}{L}\right), \tag{56}$$

with  $L$  being the correlation length and  $\sigma$  the standard deviation. The K-L expansion of the correlation for the input random temperature is performed:

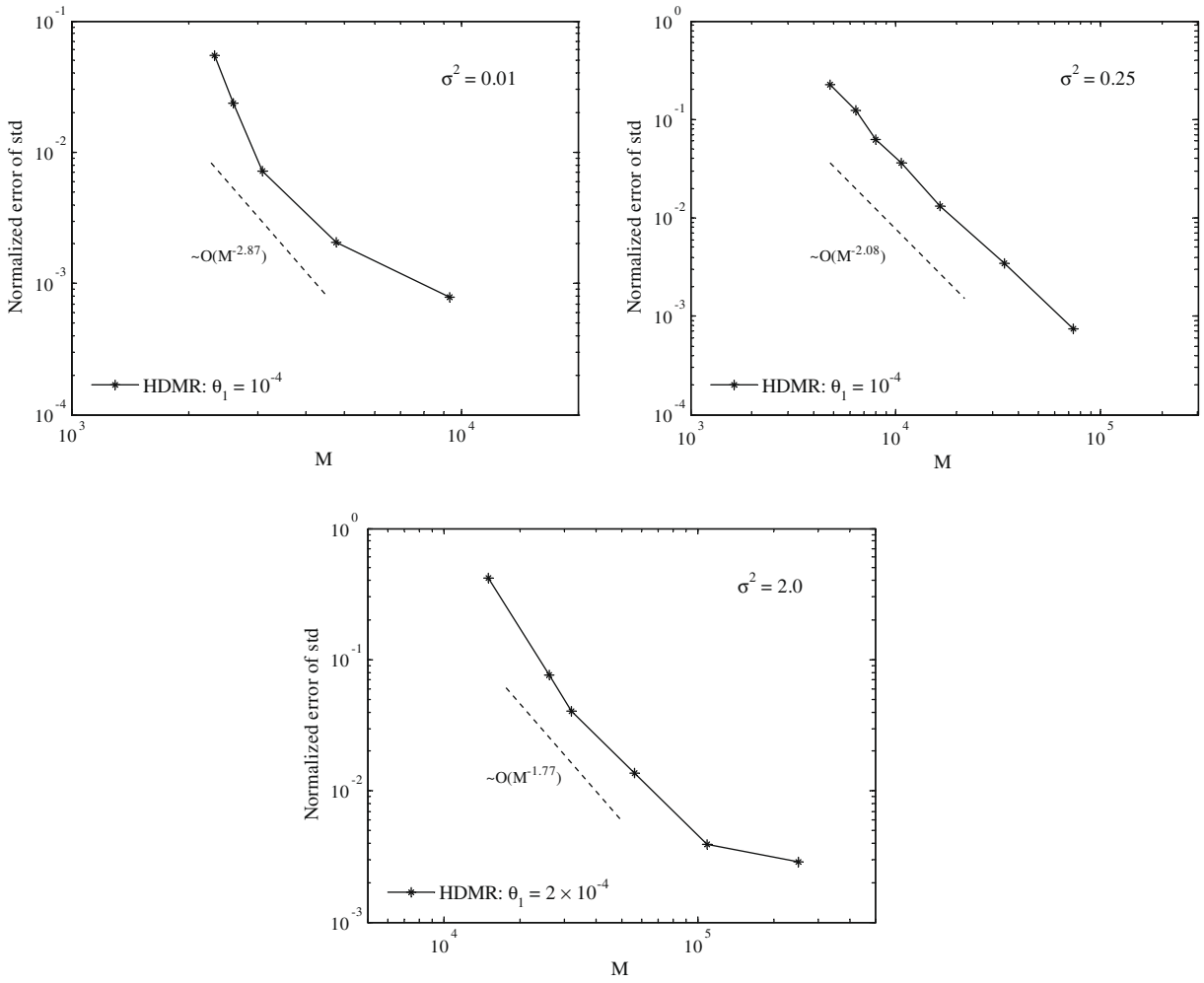


Fig. 17. Convergence of the  $L_2$  normalized errors of standard deviation of the  $v$  velocity-component for different  $\sigma^2$ , where  $L = 0.25$ .

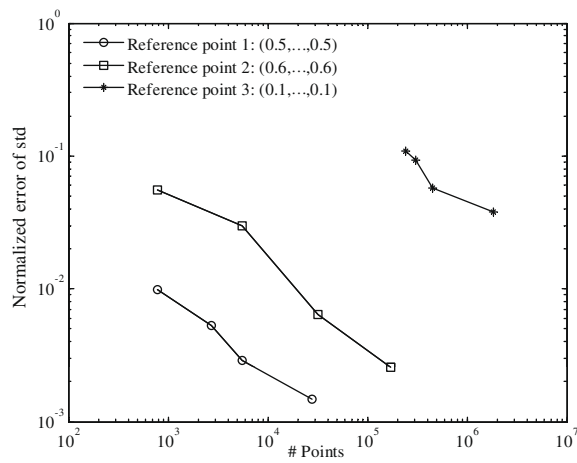


Fig. 18. Convergence of the  $L_2$  normalized errors of standard deviation of the  $v$  velocity-component for three different reference points.

$$\theta(y, \mathbf{Y}) = 0.5 + \sum_{i=1}^N \sqrt{\lambda_i} \phi_i(y) Y_i, \tag{57}$$

where the  $Y_i$  are assumed as i.i.d. uniform random variables on  $[-1, 1]$ .

**Table 8**

Comparison of performance for three different reference points.  $\varepsilon = 10^{-6}$  and  $\theta_1 = 10^{-4}$ .  $N_i$  denotes the number of important dimensions and  $p$  denotes the expansion order of the HDMR defined in Section 4.4.

$\bar{Y}$	# Terms	# Points	$N_i$	$p$
(0.5,...,0.5)	287	27968	23	2
(0.6,...,0.6)	880	170992	33	3
(0.1,...,0.1)	5526	1854460	33	4

We consider three different cases:  $L = 0.1, \sigma = 0.05, L = 0.1, \sigma = 1.0$  and  $L = 1.0, \sigma = 2.0$ . The coefficients of variation, which is the ratio of the standard deviation and the mean, are 10%, 200% and 400%, respectively. The decay rate of the eigenvalues of this correlation is much faster than the exponential one of Eq. (51). Therefore, we truncate the expansion after 10 terms, i.e. the stochastic dimension is 10. The ratio between the smallest and largest eigenvalues is  $10^{-6}$  and  $10^{-14}$  for  $L = 0.1, 1.0$ , respectively. Thus, this problem is similar to the highly anisotropic Case 2 discussed in Section 5.4. It is expected that the problem has a low effective dimensionality and a lower-order expansion may be accurate for large input variability. In addition, due to the highly anisotropic situation, the adaptive HDMR is expected to be most effective.

The mean and standard deviation of the  $v$  velocity component are shown in Fig. 19 when  $L = 0.1$  and  $\sigma = 0.05$ . We choose  $\varepsilon = 10^{-7}$  and  $\theta_1 = 10^{-4}$ . As expected, for such a small input variability, the construction of HDMR stopped after a first-order expansion even with  $\theta_1 = 10^{-4}$ . The results compare quite well with the reference solution which is from Monte Carlo simulation with  $10^5$  samples which shows that the first-order expansion is enough to capture the additive effects when each dimension is acting independently. Since the error of the mean converges very fast, we only show the convergence of error

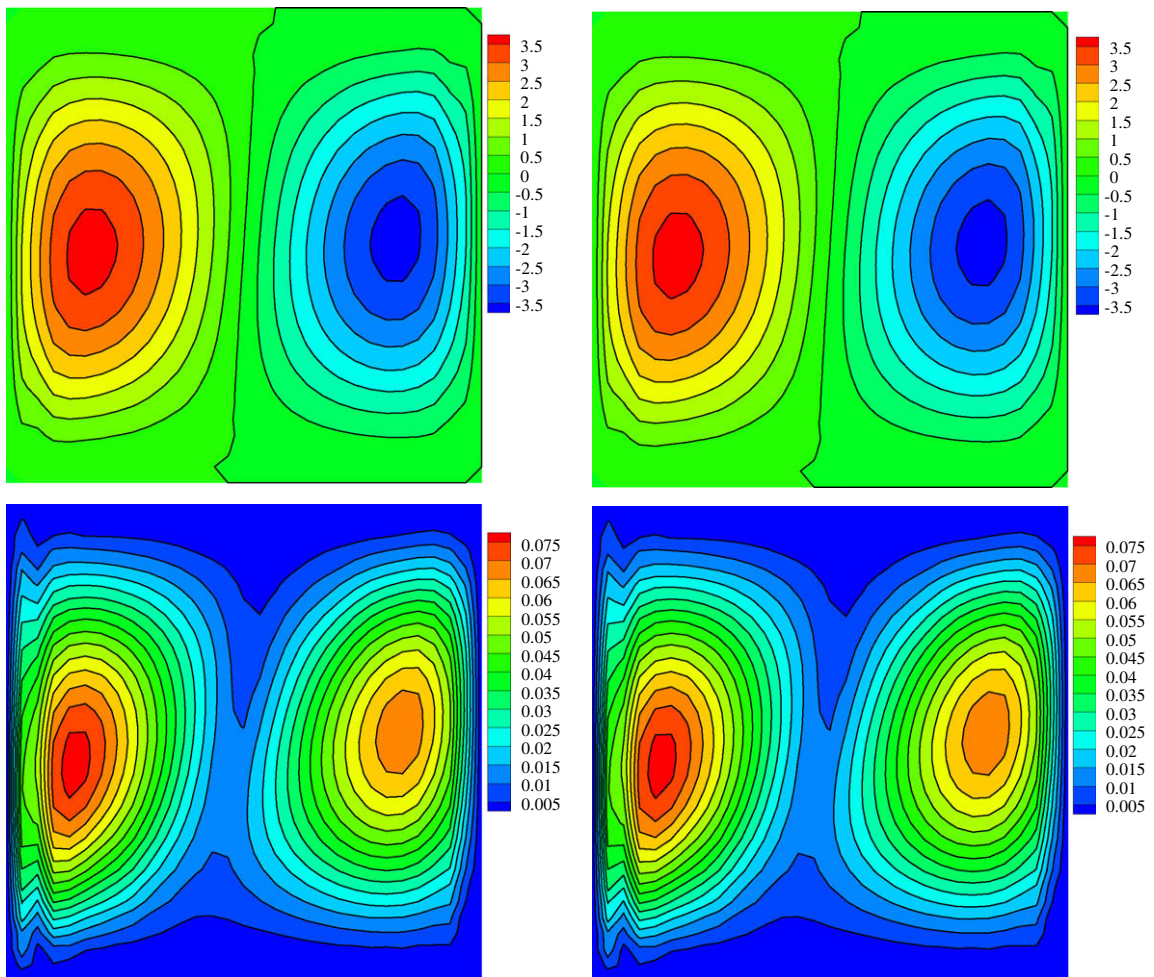


**Fig. 19.** Mean (top row) and standard deviation (bottom row) of  $v$  velocity when  $L = 0.1$  and  $\sigma = 0.05$ . Left column: HDMR solution, Right column:  $10^5$  Monte Carlo samples.

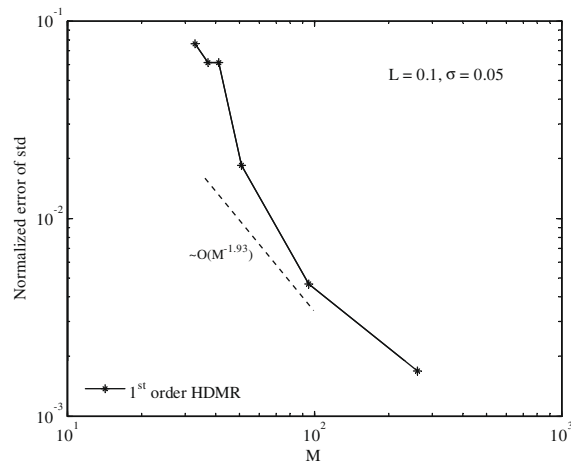


Fig. 20. Convergence of the  $L_2$  normalized errors of standard deviation of the  $v$  velocity-component where  $L = 0.1$  and  $\sigma = 0.05$ .

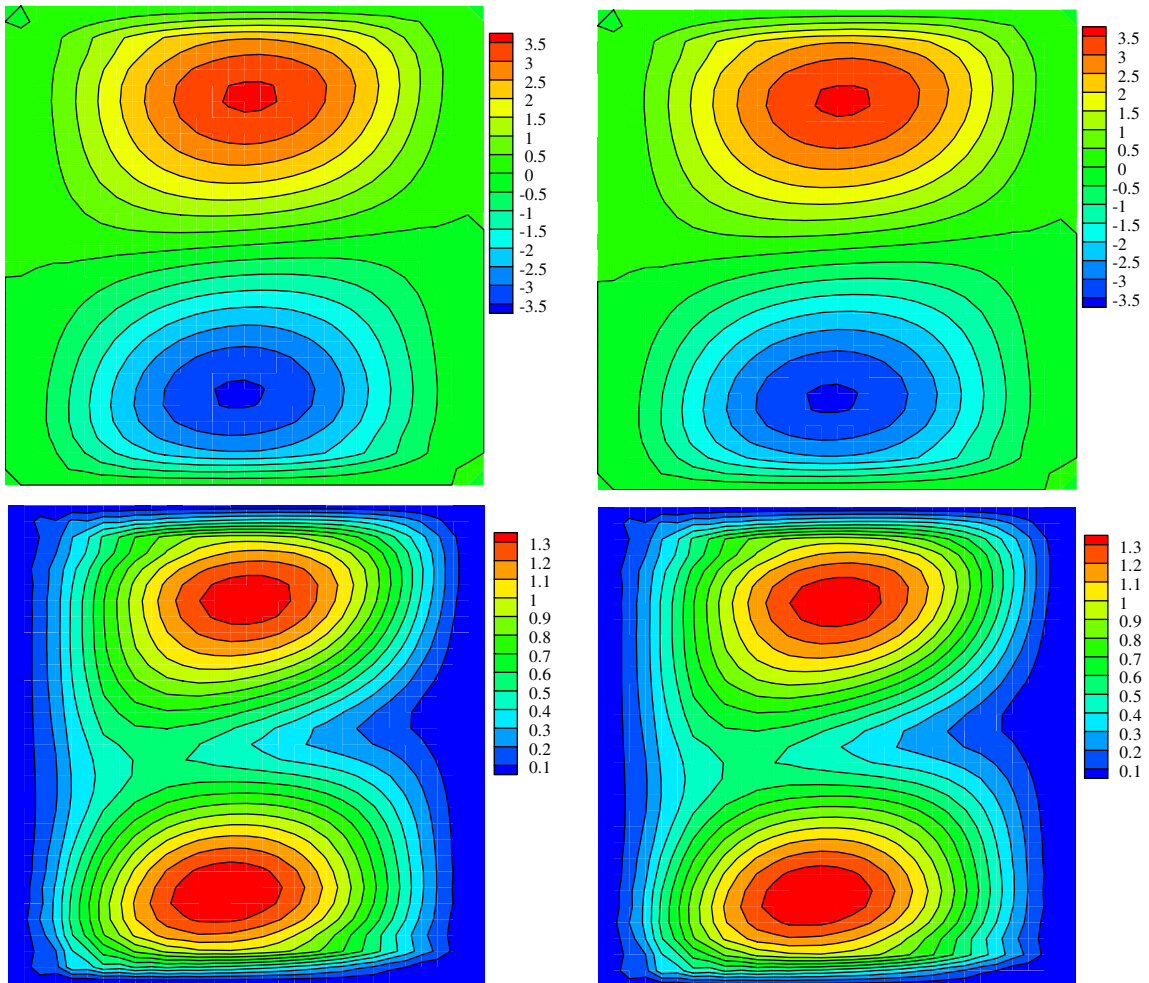


Fig. 21. Mean (top row) and standard deviation (bottom row) of  $u$  velocity when  $L = 0.1$  and  $\sigma = 1.0$ . Left column: HDMR solution, Right column:  $10^5$  Monte Carlo samples.

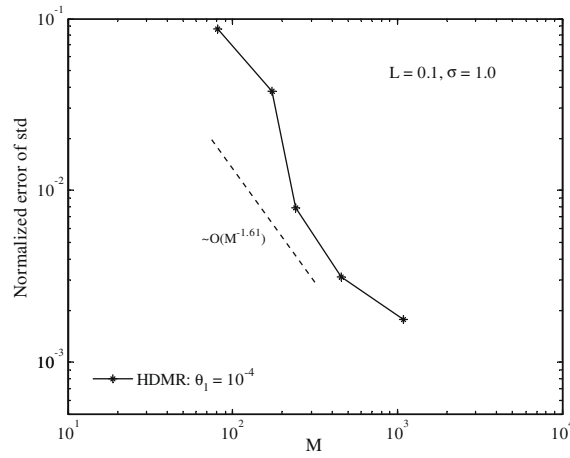


Fig. 22. Convergence of the  $L_2$  normalized errors of standard deviation of the  $u$  velocity-component where  $L = 0.1$  and  $\sigma = 1.0$ .

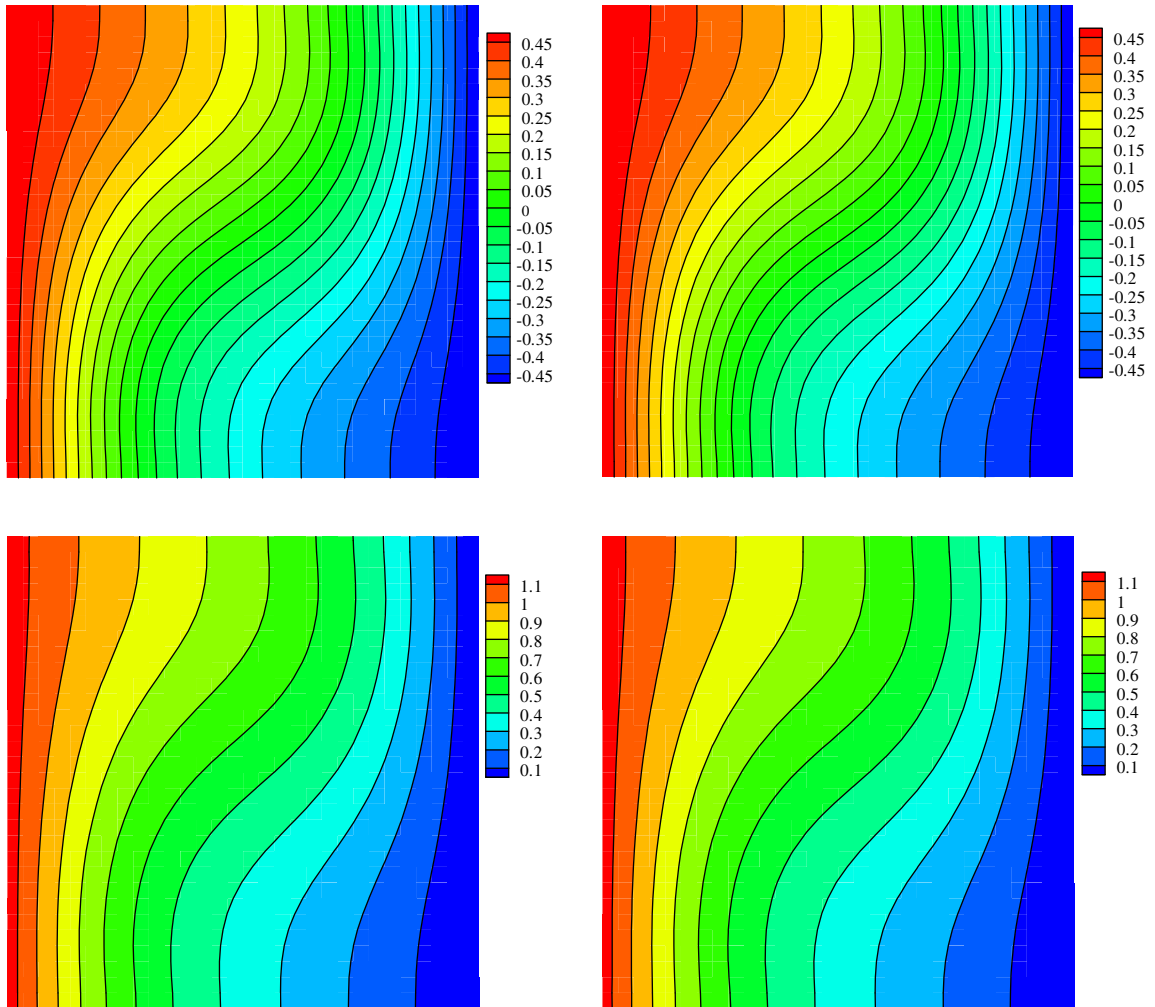


Fig. 23. Mean (top row) and standard deviation (bottom row) of temperature when  $L = 1.0$  and  $\sigma = 2.0$ . Left column: HDMR solution, Right column:  $10^5$  Monte Carlo samples.

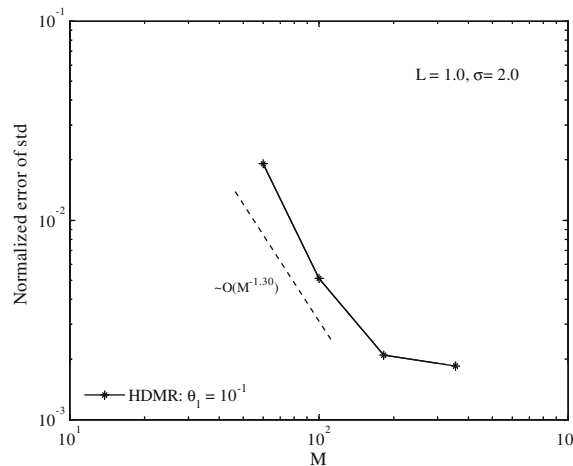


Fig. 24. Convergence of the  $L_2$  normalized errors of standard deviation of the temperature where  $L = 1.0$  and  $\sigma = 2.0$ .

of the standard deviation with decreasing  $\varepsilon$  in Fig. 20. Only 261 collocation points are needed to achieve an error  $1.69 \times 10^{-3}$ , which is a significant computational saving in comparison to MC.

Next, we consider the case  $\sigma^2 = 1.0$  and  $L = 1.0$ . For this case of high input variability, it is expected that higher-order terms are needed. We choose  $\varepsilon = 10^{-5}$  and  $\theta_1 = 10^{-4}$ . The construction stopped after order 2. However, not all the terms are needed. Only 17 component functions are in the final HDMR expansion including only 6 second-order component functions which consist of only important dimensions. The total number of terms in conventional HDMR is 56 which shows the effectiveness of the adaptive method. The mean and standard deviation of  $u$  velocity component are given in Fig. 21, which again compares well with the MC results. The error convergence is shown in Fig. 22. Only 1085 collocation points are needed to achieve an error  $1.78 \times 10^{-3}$ . It is noted that the convergence rate is a little slower than that of  $\sigma = 0.05$ , which is consistent with Fig. 17.

Finally, we consider the extreme case  $L = 1.0$  and  $\sigma = 2.0$ . It is noted that this case may be not feasible in physical sense. However, we still include it to demonstrate the applicability of this method. We choose  $\varepsilon = 10^{-5}$  and  $\theta_1 = 0.1$  such that only the first two dimensions are important. Only 356 collocation points are required to obtain a good comparison with that of MC results, which is shown in Fig. 23. The only second-order component function is  $f_{12}$ . By adding this term to the first-order expansion, the error of temperature standard deviation decreases from  $3.25 \times 10^{-3}$  to  $1.86 \times 10^{-3}$ . This example clearly demonstrates the significance of including the important component function which captures the strong correlation effects among important dimensions. The error convergence is given in Fig. 24.

## 6. Conclusions

In this paper, a novel adaptive high-dimensional stochastic model representation technique for solving high-dimensional SPDEs is introduced. This method applies HDMR in the stochastic space and decomposes the original  $N$ -dimensional problem into several low-dimensional sub-problems. This has been shown to be more efficient than solving the  $N$ -dimensional problem directly. Each sub-problem is solved using ASGC, where a proper error indicator is introduced to adaptively refine locally the collocation points.

Numerical examples involving both elementary mathematical functions and stochastic fluid mechanics problems have been conducted to verify the accuracy and efficiency of the proposed method. The numerical examples show that the number of component functions needed in the HDMR expansion for a fixed stochastic dimension depends both on the input variability and the important dimensions no matter how many stochastic dimensions there are. However, it does not depend on the type of the function, i.e. whether the SPDE is linear or nonlinear. Although, in general, lower-order expansion is enough to capture all the input uncertainty to a good accuracy, the number of component functions increases quickly with the dimension. It is impossible to calculate all the terms through conventional HDMR in the case of extremely high-stochastic dimension. However, by using the adaptive version of HDMR, we can effectively solve the problem within a desired accuracy even for problems with high-dimensional high input variability. On the other hand, for small variability, the first-order expansion is accurate enough. Therefore, the HDMR is quite suitable in most real physical applications for simulating high-dimensional stochastic problems in the area of uncertainty quantification where the correlation length is small and the input variability is generally large and solving the  $N$ -dimensional problem directly by ASGC is not feasible. It is also shown that the convergence rate of the proposed method is even better than that of MC for the problems considered up to 500 stochastic dimensionality.

Finally, we note that the proposed method is more computationally efficient than applying the ASGC method directly on the function of interest or to represent the solution of an SPDE. This is due mainly to the fact that implementation of HDMR

requires less memory storage and avoids the heavy surplus calculation typical of high-dimensional problems. However, it is emphasized that HDMR may not be of practical use for interpolating arbitrary mathematical functions where sometimes all  $2^N$  terms might be required, for example, in the case of a function with multiplicative nature.

## Acknowledgments

This research was supported by the Computational Mathematics Program of AFOSR (Grant F49620-00-1-0373), the Computational Mathematics Program of the NSF (Award DMS-0809062) and an OSD/AFOSR MURI-09 award on uncertainty quantification.

## References

- [1] R. Ghanem, P.D. Spanos, *Stochastic Finite Elements: A Spectral Approach*, Springer-Verlag, New York, 1991.
- [2] B. Ganapathysubramanian, N. Zabarav, Modeling diffusion in random heterogeneous media: data-driven models, stochastic collocation and the variational multiscale method, *J. Comput. Phys.* 226 (2007) 326–353.
- [3] B. Ganapathysubramanian, N. Zabarav, A non-linear dimension reduction methodology for generating data-driven stochastic input models, *J. Comput. Phys.* 227 (2008) 6612–6637.
- [4] D. Zhang, *Stochastic Methods for Flow in Porous Media: Coping with Uncertainties*, Academic Press, San Diego, CA, 2002.
- [5] D. Zhang, Z. Lu, An efficient, high-order perturbation approach for flow in random porous media via Karhunen–Loève and polynomial expansions, *J. Comput. Phys.* 194 (2004) 773–794.
- [6] Z. Lu, D. Zhang, A comparative study on uncertainty quantification for flow in randomly heterogeneous media using Monte Carlo simulations and conventional and KL-based moment-equation approaches, *SIAM J. Sci. Comput.* 26 (2004) 558–577.
- [7] D. Xiu, G.E. Karniadakis, The Wiener–Askey polynomial chaos for stochastic differential equations, *SIAM J. Sci. Comput.* 24 (2002) 619–644.
- [8] R. Ghanem, Probabilistic characterization of transport in heterogeneous media, *Comput. Methods Appl. Mech. Eng.* 158 (1998) 199–220.
- [9] D. Xiu, G.E. Karniadakis, Modeling uncertainty in steady state diffusion problems via generalized polynomial chaos, *Comput. Methods Appl. Mech. Eng.* 191 (2002) 4927–4948.
- [10] D. Xiu, G.E. Karniadakis, A new stochastic approach to transient heat conduction modeling with uncertainty, *Int. J. Heat Mass Trans.* 46 (2003) 4681–4693.
- [11] B. Velamuri Asokan, N. Zabarav, A stochastic variational multiscale method for diffusion in heterogeneous random media, *J. Comput. Phys.* 218 (2006) 654–676.
- [12] X. Ma, N. Zabarav, A stabilized stochastic finite element second-order projection method for modeling natural convection in random porous media, *J. Comput. Phys.* 227 (2008) 8448–8471.
- [13] I. Babuska, R. Tempone, G.E. Zouraris, Galerkin finite element approximations of stochastic elliptic partial differential equations, *SIAM J. Numer. Anal.* 42 (2004) 800–825.
- [14] D. Xiu, J.S. Hesthaven, High-order collocation methods for differential equations with random inputs, *SIAM J. Sci. Comput.* 27 (2005) 1118–1139.
- [15] D. Xiu, Efficient collocation approach for parametric uncertainty analysis, *Commun. Comput. Phys.* 2 (2007) 293–309.
- [16] I. Babuska, F. Nobile, R. Tempone, A stochastic collocation method for elliptic partial differential equations with random input data, *SIAM J. Numer. Anal.* 45 (2007) 1005–1034.
- [17] F. Nobile, R. Tempone, C. Webster, A sparse grid stochastic collocation method for partial differential equations with random input data, *SIAM J. Numer. Anal.* 46 (2008) 2309–2345.
- [18] B. Ganapathysubramanian, N. Zabarav, Sparse grid collocation schemes for stochastic natural convection problems, *J. Comput. Phys.* 225 (2007) 652–685.
- [19] F. Nobile, R. Tempone, C. Webster, An anisotropic sparse grid stochastic collocation method for partial differential equations with random input data, *SIAM J. Numer. Anal.* 46 (2008) 2411–2442.
- [20] S. Smolyak, Quadrature and interpolation formulas for tensor product of certain classes of functions, *Soviet Math. Dokl.* 4 (1963) 240–243.
- [21] B. Ganapathysubramanian, N. Zabarav, A stochastic multiscale framework for modeling flow through heterogeneous porous media, *J. Comput. Phys.* 228 (2009) 591–618.
- [22] B. Ganis, H. Klie, M. Wheeler, T. Wilder, I. Yotov, D. Zhang, Stochastic collocation and mixed finite elements for flow in porous media, *Comput. Methods Appl. Mech. Eng.* 197 (2008) 3547–3559.
- [23] X. Ma, N. Zabarav, An adaptive hierarchical sparse grid collocation method for the solution of stochastic differential equations, *J. Comput. Phys.* 228 (2009) 3084–3113.
- [24] H. Rabitz, Ö.F. Aliş, J. Shorter, K. Shim, Efficient input–output model representations, *Comput. Phys. Commun.* 117 (1999) 11–20.
- [25] H. Rabitz, Ö.F. Aliş, General foundations of high-dimensional model representations, *J. Math. Chem.* 25 (1999) 197–233.
- [26] Ö.F. Aliş, H. Rabitz, Efficient implementation of high dimensional model representations, *J. Math. Chem.* 29 (2001) 127–142.
- [27] S.W. Wang, H. Levy II, G. Li, H. Rabitz, Fully equivalent operational models for atmospheric chemical kinetics within global chemistry-transport models, *J. Geophys. Res.* 104 (1999) 30417–30426.
- [28] G. Li, C. Rosenthal, H. Rabitz, High dimensional model representation, *J. Phys. Chem. A* 105 (2001) 7765–7777.
- [29] I.M. Sobol, Theorems and examples on high dimensional model representation, *Reliab. Eng. Syst. Saf.* 79 (2003) 187–193.
- [30] G. Li, S.W. Wang, H. Rabitz, S. Wang, P. Jaffe, Global uncertainty assessments by high dimensional model representations (HDMR), *Chem. Eng. Sci.* 57 (2002) 4445–4460.
- [31] S. Balakrishnan, A. Roy, M.G. Ierapetritou, G.P. Flach, P.G. Georgopoulos, A comparative assessment of efficient uncertainty analysis techniques for environmental fate and transport models: application to the FACT model, *J. Hydrol.* 307 (2005) 204–218.
- [32] S. Rahman, H. Xu, A univariate dimension-reduction method for multi-dimensional integration in stochastic mechanics, *Probab. Eng. Mech.* 19 (2004) 393–408.
- [33] H. Xu, S. Rahman, A generalized dimension-reduction method for multidimensional integration in stochastic mechanics, *Int. J. Numer. Meth. Eng.* 61 (2004) 1992–2019.
- [34] H. Xu, S. Rahman, Decomposition methods for structural reliability analysis, *Probab. Eng. Mech.* 20 (2005) 239–250.
- [35] S. Rahman, A dimensional decomposition method for stochastic fracture mechanics, *Eng. Fract. Mech.* 73 (2006) 2093–2109.
- [36] R. Chowdhury, B.N. Rao, A.M. Prasad, High-dimensional model representations for structural reliability analysis, *Commun. Numer. Methods Eng.* 25 (2009) 301–337.
- [37] J. Foo, G.E. Karniadakis, Multi-element probabilistic collocation method in high dimensions, *J. Comput. Phys.* 229 (2010) 1536–1557.
- [38] M. Griebler, M. Holtz, Dimension-wise Integration of High-dimensional Functions with Applications to Finance, *INS Preprint NO. 0809*, November 2008.
- [39] B. Oksendal, *Stochastic Differential Equations: An Introduction with Applications*, Springer-Verlag, New York, 1998.
- [40] F.Y. Kuo, I.H. Sloan, G.W. Wasilkowski, H. Woźniakowski, On the Decompositions of Multivariate Functions, *Math. Comput.* 270 (2010) 953–966.

- [41] X. Wang, On the approximation error in high dimensional model representation, in: *Proceedings of the 2008 Winter Simulation Conference*, 2008, pp. 453–462.
- [42] X. Ma, N. Zabarar, An efficient Bayesian inference approach to inverse problems based on adaptive sparse grid collocation method, *Inverse Probl.* 25 (2009) 035313. 27pp.
- [43] A. GENZ, A package for testing multiple integration subroutines, in: *Numerical Integration: Recent Developments, Software and Applications*, 1987, pp. 337–340.